Maximal and Pseudo-Maximal Wave Concepts for Freak Waves Applied to the Draupner Wave

AL. Latifah

Department of Applied Mathematics

Universiteit Twente

A thesis submitted for the degree of

Master of Science (MSc)

Supervisor: Prof. Dr. E.W.C van Groesen

Day of the defense: 31 May 2010

Contents

List of Figures

1

Introduction

Freak waves are extreme waves that occur relatively seldom, but can cause severe damages to ships in the ocean. One damage example of freak waves is the accident of Ship "Voyager" on 14 February 2005 [1]. The ship came across a severe storm and was hit by one or more high waves. It is observed that freak waves often occur not only in the area whose severe storm, but also in the area where waves propagate into a strong opposing current, for example in the "Agulhas" current outside South Africa [3]. The strong current going south meets strong swell from storms in the Antarctic Ocean, therefore many large ships have encountered difficulties in that area.

In the last decade many scientists work on freak waves. They focus on many different aspects of freak waves, such as the frequency or the probability of occurrence of freak waves, the effects of wind on the freak waves, the wave distribution, the statistical properties of surface gravity waves, the spectral characteristics of waves, risk analysis on wave crest kinematics, the implication of freak waves for marine safety, etc.

Interesting questions that need to be answered in the research of freak waves are how high is the highest wave, which properties does a freak wave have, how often and under what circumstances do freak waves occur, and what are the physical effects of freak waves that lead to such a focusing of wave energy in the open ocean. According to [3] there are three possible physical effects that can lead to freak waves: focusing in time and in space, current focusing, and nonlinear focusing. The first two are described by so-called linear theory and have been known since the beginning of the past century.

- Focusing in time and space
  This effect is used in large wave tanks to generate very high wave to test ships in extreme weather situations. With a wave maker at the end of the tank one designs a signal in the form of a wave train where the wave length varies, with the shortest waves in front. Long waves propagate faster and will catch up with the shorter waves. Focussing of this train creates a few large waves over a short time and within a limited area.

- Current focusing
  Even though the current velocities in the open ocean (far from coastal areas) are small, typically about 10[cm/s], they can give small deflections of the waves when they act over long distances [3]. The deflection due to the current produces areas of increased and areas of decreased wave intensity. The result can be local focusing or defocusing of wave energy. This has been proposed as an explanation of freak waves by White and Fornberg [25].

- Nonlinear focusing
  As opposed to the effects above, this one cannot be explained by linear theory. It was shown in the middle of the 1960s that if we generate uniform periodic waves in one end of a long wave tank, the waves will spontaneously split into groups, which get more prominent as they propagate along the tank [3]. According to linear theory these waves should remain uniform and periodic. One developed a wave equation (the so-called nonlinear Schrödinger equation) capable of explaining this strange behavior qualitatively. This equation has later been modified and improved to also give good quantitative agreement with experiments. The phenomenon of freak waves is essentially nonlinear. This justified the use of nonlinear Schrödinger equation as candidate to explain freak waves [3]. The AB equation derived by van Groesen and Andonowati [22] is a novel wave equation that accurately models the nonlinearity of water waves. Consequently, this equation can be used to try to explain freak waves. In this thesis we would rather apply AB equation than nonlinear Schrödinger equation since the Schrödinger equation only computes the envelope of a wave group.

There are mainly two approaches that are used for the description of water waves: the deterministic (physical) approach and the statistical one [12]. Compared to the statistical methods, the physical analysis of freak waves is much less developed than the statistical analysis. In the Conference proceedings of rogue waves 2008, approximately 30% of the papers discussed about physical aspects of freak waves and some were not yet employed for the analysis of freak waves clearly [6]. This indicates that the physics of freak waves is still poorly understood. One reason for this will be that there are only very few reliable data available since it is very rare to detect one in the various types of surface wave data.

Despite much research in the past two decades, not much is known yet about the mechanisms that lead to the appearance of freak waves. This thesis contributes to study the mechanism of freak waves. To that end we will use data of one well known freak wave, the so-called New Year's Wave or Draupner wave. The information of the Draupner wave is used in the deterministic-stochastic investigations of freak waves in this thesis. Walker *et al.* [24] define a convenient 'design wave' based on the average shape of an extreme wave in a linear Gaussian process to reproduce the Draupner Wave. This design is known as NewWave. In addition to this, we introduce 'maximal', and 'pseudo-maximal' waves as new concepts, and test the applicability. Numerical simulations with the AB equation provide additional insights in the spatial evolution.

The structure of this thesis consists of five chapters, starting with this Introduction. In Chapter 2 part of the literature about freak waves is summarised and the Draupner wave is presented. In addition the so-called NewWave is described. The maximal wave and the pseudo-maximal wave are introduced as new concepts in Chapter 3. The explanation of the AB equation and the spatial evolution of the Draupner wave with the AB equation are presented in Chapter 4. Chapter 5 contains conclusions and recommendations. Some technical details can be found in the appendices.

1. INTRODUCTION

2

Freak Waves in the ocean

2.1 Definition of Freak Waves

Before introducing a freak wave, we first illustrate some properties of a wave that we will use further. Look at Figure 2.1.

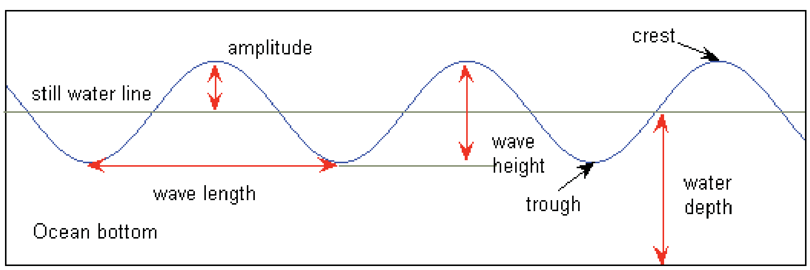

Figure 2.1: Some properties of a wave

Freak waves were first recognized by Draper [2] four and a half decades ago. Freak waves are waves of extreme, unexpectedly large height that suddenly appear in a relatively mild background wave field. Sometimes freak waves are also known as rogue waves, extreme waves, or giant waves [18]. In the last decade, freak waves have become an important study topic in engineering and science. The most common definition of a freak wave is a wave for which the ratio of wave height to significant wave height exceeds 2.2 (see [7, 11]). The definition of significant wave height is given in section 2.2. Uggo Ferreira [4] defines a freak wave as a particular kind of ocean wave that displays a singular, unexpected wave profile characterized by an extraordinary large and steep crest or trough.

Another definition is based on a statistical approach. Haver [7] defines a freak wave as an event that represents an outlier when seen in view of the population of events generated by a piecewise stationary and homogeneous second order model of the surface process. This second order model is explained by Forristal [5] (see also [13], [21]). In general, a freak event is an event that would not be expected under the typical engineering models for extreme wave predictions. In this thesis we consider the definition of an extreme wave according to the ratio of wave height to significant wave height.

2.2 Introduction to the Draupner Wave

On January 1st 1995, an extreme wave was measured under the Draupner platform (16/11-E) providing indisputable evidence that such waves do indeed exist [24, 12]. The Draupner platform is located in the North Sea off the coast of Norway in water of 70[m] depth. The bathymetry of the North sea can be observed in Figure 2.2. The precise location of the Draupner platform is 58.11^0N; 2.28^0E [19] (see the cross line in Figure 2.2).

The weather situation at that time can be seen in Figure 2.3. The weather pattern is dominated by a major low with center in Southern Sweden causing a strong northerly wind field over the whole North sea and Norwegian sea [8]. In addition a smaller low moved southwards in the North sea during the morning hours and the effect of this smaller low is to strengthen the wind field in the western North sea. Therefore the area with the strongest wind field moved southwards as indicated in Figure 2.3. The wind conditions seemed to peak at hurricane level wind between 12 GMT and 18 GMT [8]. In Figure 2.3 the Draupner platform is indicated by red rectangular. It is shown that the platform was outside the area where the wind conditions seem to have been most extreme.

Minor damage was inflicted on the platform during the extreme wave event, confirming the validity of the reading made by a downwards-pointing laser sensor. In an area with

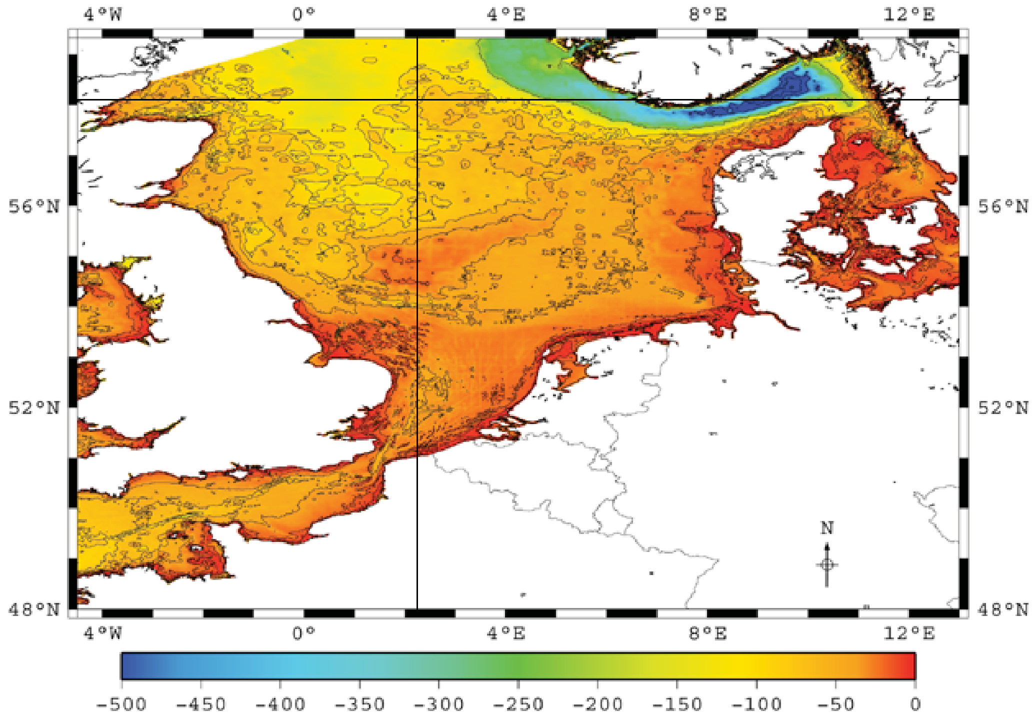

Figure 2.2: The bathymetry of North sea. The Draupner platform is at the cross lines. Image source `http://amcg.ese.ic.ac.uk/` [27]

significant wave height (a well-defined and standardized statistic quantity to denote the characteristic height of the random waves which is computed by the average wave height of the one-third largest waves) of approximately 12 metres, a freak wave with a maximum wave height of 25.6 metres occurred (peak elevation was 18.5 metres). This freak wave recorded with starting time 15:20 GMT has been known in the international scientific community as the New Year's wave or Draupner wave. The other statistical parameters of this waves record are the mean and variance. These can be computed by the definition of mean and variance (see Appendix A). The mean of the amplitude of this waves record is approximately zero and the variance is 8.88. This can be observed in Figure 2.6. This figure also shows that the amplitude of 18.5[m] is an outlier.

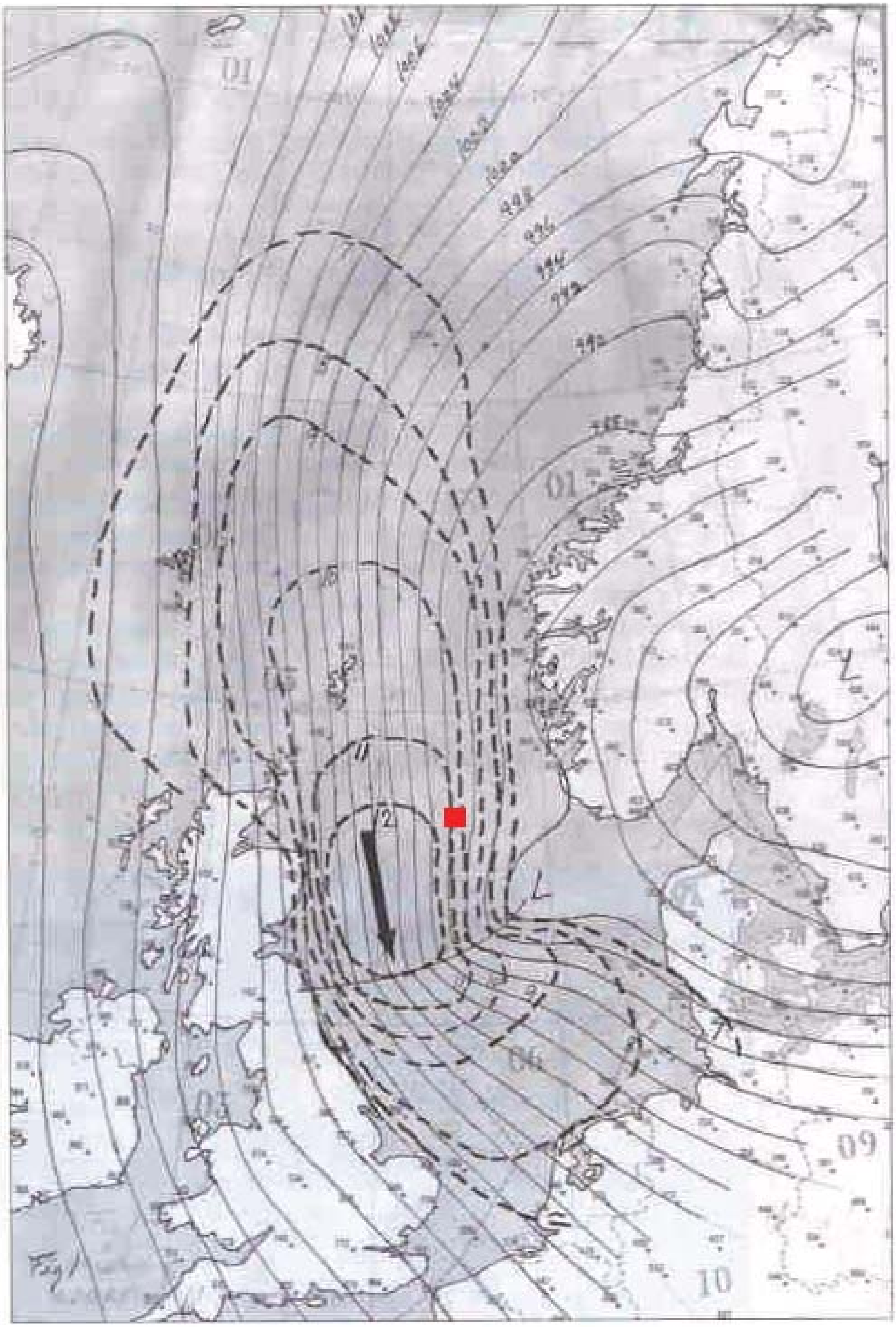

Figure 2.3: The weather situation in North Sea, 1 January 1995 at 12 GMT. Image source: Haver [8]

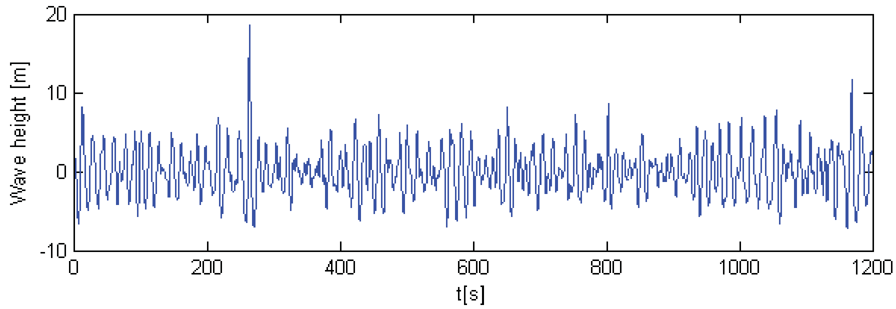

Figure 2.4: Full time series signal recorded from the Draupner platform on 1st January 1995

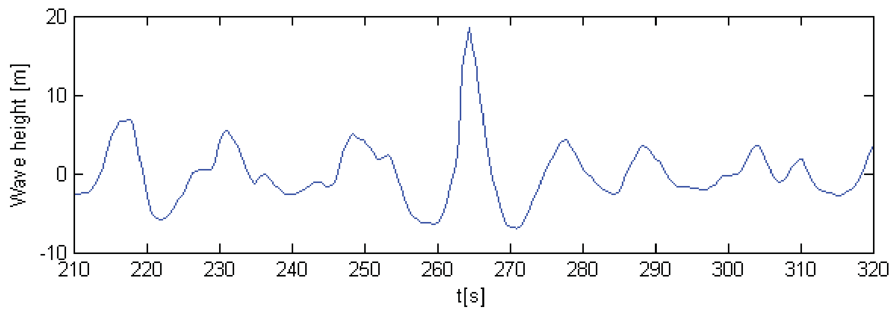

Figure 2.5: A closer look of the freak wave event

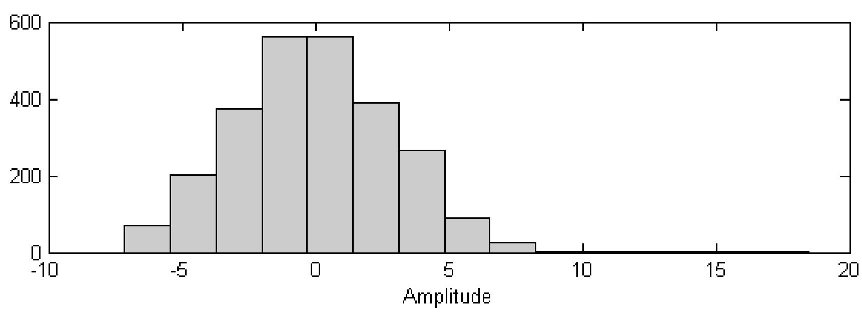

Figure 2.6: Histogram of the amplitude of the signal record

A 20-minutes surface wave elevation time series of the Draupner signal is shown in Figure 2.4 with a closer look of the freak event in Figure 2.5. There are approximately 100 waves in the record. Walker *et al.* [24] have shown that the Draupner wave displays nonlinear behaviour. The shapes of the crests are consistently sharper and larger than their corresponding troughs. They proved the nonlinear behaviour by showing the asymmetry between crests and troughs since it is the most obvious manifestation of nonlinearity in the ocean.

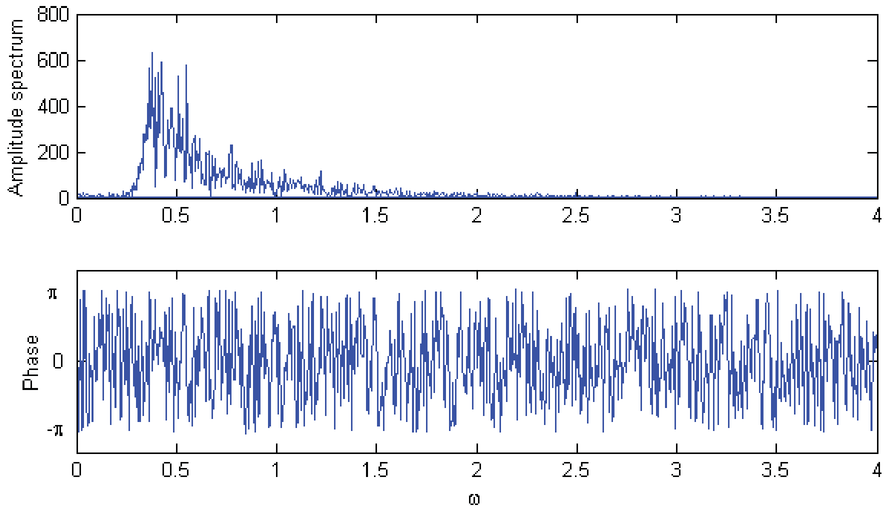

Figure 2.7: The spectrum and the phases of the full time series Draupner signal

As additional information, we show the amplitude spectrum and the phases of the full time series Draupner signal. The amplitude spectrum describes the amplitude distribution as a function of the frequencies. It is defined by the absolute value of the Fourier transform of a signal. Given a signal $s(t)$, then the amplitude spectrum, $|\breve{s}(\omega)|$, is formulated by:

$$|\breve{s}(\omega)| = \frac{1}{2\pi} \left| \int s(t) e^{i\omega t} dt \right| \tag{2.1}$$

Further we will also use the power spectrum, $S(\omega)$, which is the squares of the amplitude spectrum, i.e. $S(\omega) = |\breve{s}(\omega)|^2$. Figure 2.7 shows that the amplitude spectrum is dominant in $0.25 < \omega < 0.9$ (we plotted the spectrum until $\omega = 4$ and zoomed it for $0.25 \leqslant \omega \leqslant 0.9$). The lower plot in Figure 2.7 shows the phases of the Draupner signal. To know how the phases are distributed, we observe the histogram of the Draupner phases for positive ω in Figure 2.9. This figure shows that the phases are random in

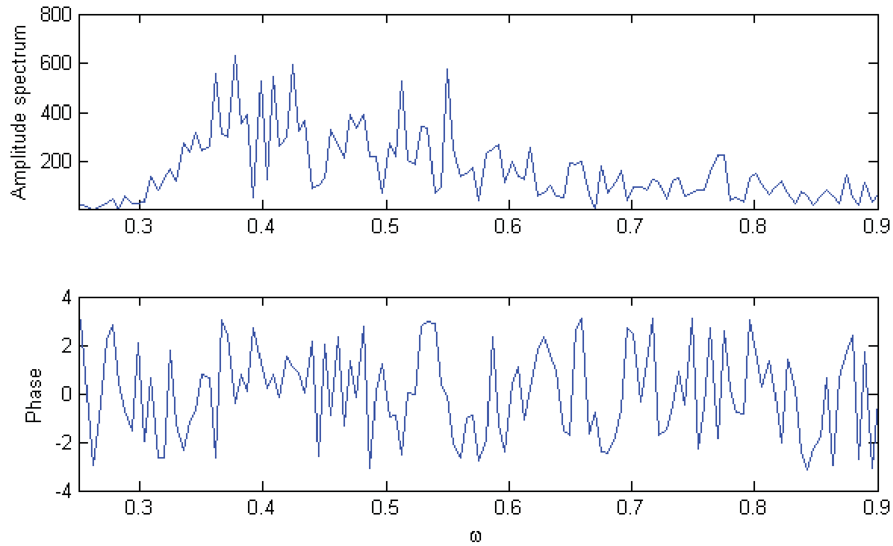

Figure 2.8: The zoomed version of Figure 2.7

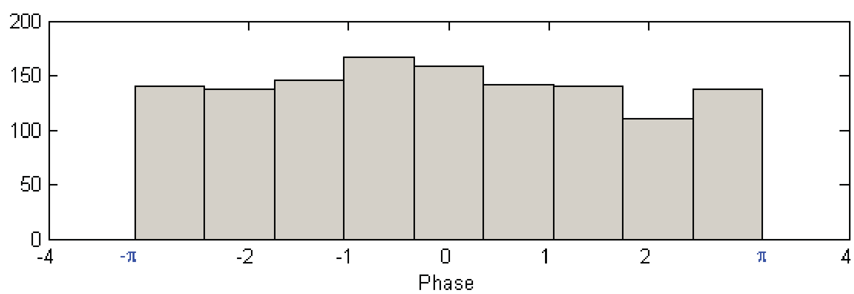

Figure 2.9: Histogram of the Draupner phases (full time series)

the range $[-\pi, \pi]$, therefore this can be estimated by uniform distribution. The maximum of the Draupner phases is 3.14 (approximately π) and the minimum is -3.1408 (approximately $-\pi$). The average of the Draupner phases is -0.0691 and the variance is 3.1615 (standard deviation, $\sigma = 1.77 = 0.56\pi$). In this thesis we will not use this full time series of the Draupner signal, but we only use small interval of the Draupner signal as defined in the next section.

2.3 Draupner signal for simulation

Without restriction the Draupner wave is assumed to be a generated wave at position $x = 0$. It is 1200[s] time signal and the maximal crest height happened at time 264.4[s]. Without restriction we take the maximal crest height at $t = 0$ and consider a symmetric interval around $t = 0$. Hence, we do not use the full time series Draupner signal, but take the first 528.8[s] of the signal so that the maximal crest height is at $t = 0$. See Figure 2.10. The amplitude spectrum and its phases are presented in Figure 2.11.

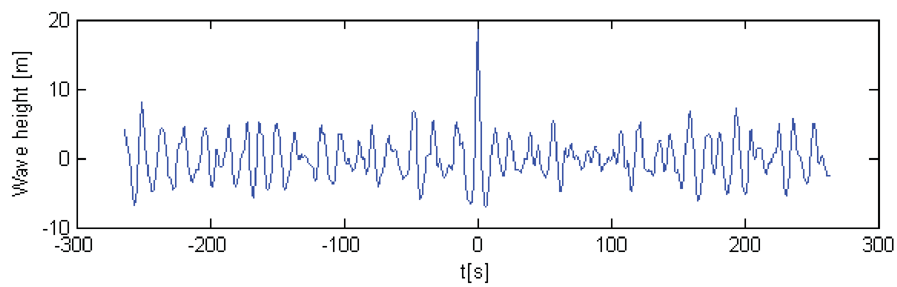

Figure 2.10: $s(t)$, the time signal which we use for the simulation

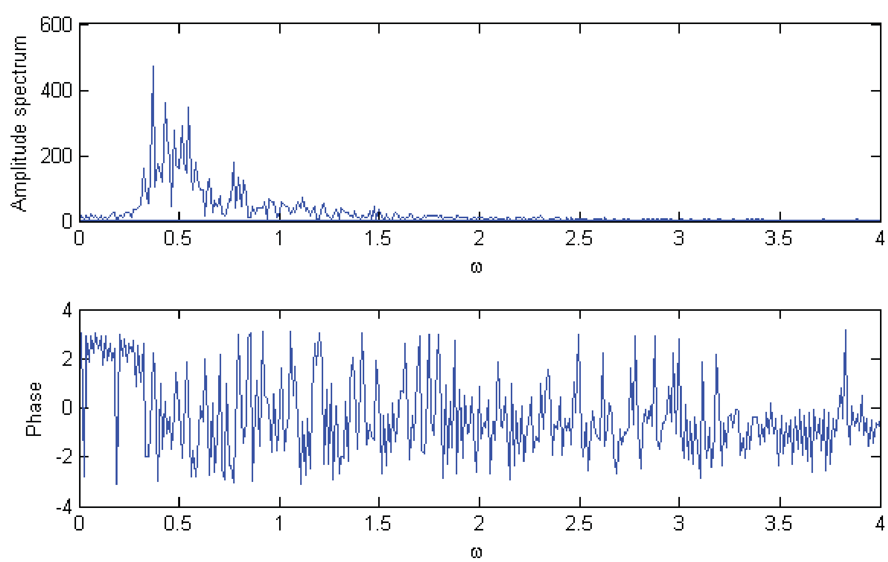

Figure 2.11: The amplitude spectrum and the phases of Draupner signal (small interval)

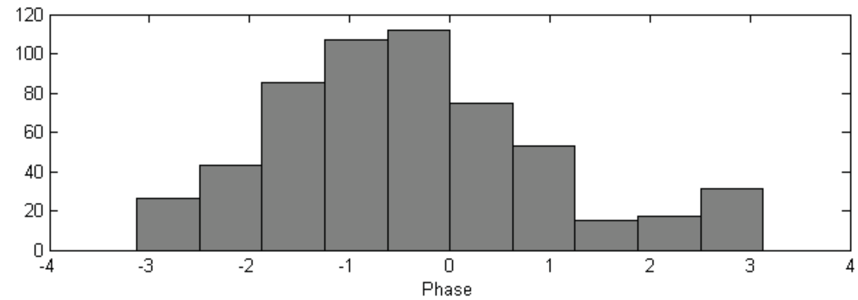

Figure 2.12: Histogram of the Draupner phases (small interval)

The amplitude spectrum is indeed not the same as the amplitude spectrum of the full Draupner signal since we cut the signal for $t > 528.8$[s], but it is still dominant in $0.25 < \omega < 0.9$. Meanwhile the phases are in the range $(-\pi, \pi)$ and are no longer uniformly distributed. This can be observed from the histogram in Figure 2.12. The distribution of the phases concentrates to the left (skew positive). The maximum of the phases is 3.13 and the minimum is -3.13. The mean of the phases is -0.38 and the variance is 1.89 (standard deviation, $\sigma = 0.44\pi$).

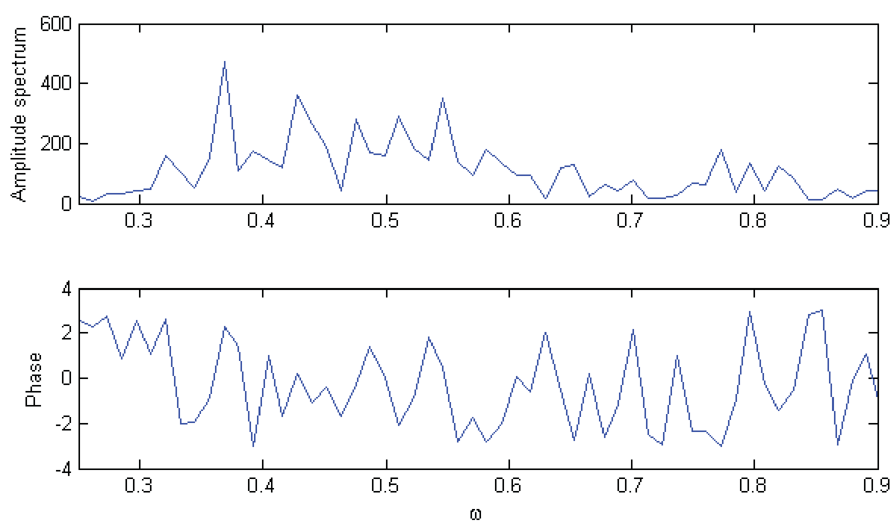

Figure 2.13: The zoomed version of Figure 2.11

Since the amplitude spectrum is dominant in $0.25 < \omega < 0.9$, now we observe the

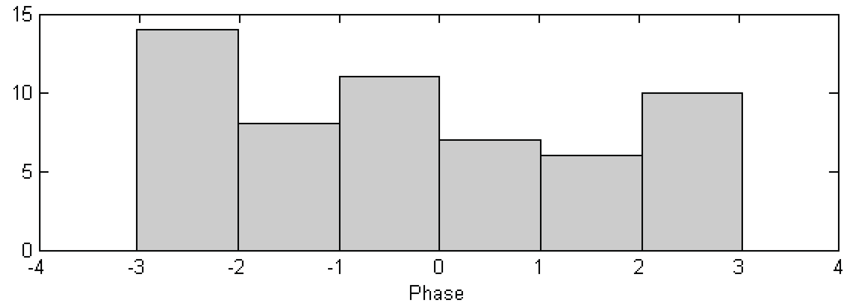

Figure 2.14: Histogram of the Draupner phases for $0.25 < \omega < 0.9$ (small interval)

phases in this ω range (see Figure 2.13 and the histogram in Figure 2.14). The phases are quite random. The maximum of the phases is 3.04 and the minimum is -3.02. The mean of the phases is -0.27 and the variance is 3.63 (standard deviation, $\sigma = 0.61\pi$). This kind of phases will be employed as the motivation to define pseudo-maximal wave later in section 3.3.1.

2.4 Statistical properties of wave dynamics

Generally, sea waves behave irregularly and unpredictably in even rather short time scales, although they show some periodicity. Therefore, the dynamical system in the ocean can be modelled as random wave dynamics. The sea surface elevation at one moment of time t_0 in one point x_0 is represented by the random function numbered by the index j: $\eta_j(x_0, t_0)$ with some statistical properties [12]. This is the approach to study models of the evolution of statistical wave dynamics. Suppose we have the surface elevation $\eta(x,t)$, as a function of space and time. Since we are mainly concerned with the temporal profiles, we write $\eta(t)$ instead of $\eta(x,t)$. To evaluate the cross correlation of the profiles with themselves, we make use of the autocorrelation. The autocorrelation is defined as the expected value of the product of a signal with the time-shifted version of itself, at lag τ:

$$R_{\eta\eta}(\tau) = \int \eta(t)\overline{\eta}(t-\tau)dt. \tag{2.2}$$

where $\overline{\eta}$ denotes the complex conjugate of η. For a real function, $\overline{\eta} = \eta$. Applying Parseval's theorem and Fourier properties to the autocorrelation definition we obtain that the autocorrelation is the Fourier transform of the power spectrum of the signal

$$\begin{aligned} R_{\eta\eta}(\tau) &= \int \eta(t)\overline{\eta}(t-\tau)dt \\ &= \int \breve{\eta}(\omega)\overline{\breve{\eta}}(\omega)e^{-i\omega\tau}d\omega \\ &= \int |\breve{\eta}(\omega)|^2 e^{-i\omega\tau}d\omega \end{aligned} \tag{2.3}$$

in which $|\breve{\eta}(\omega)|$ is amplitude spectrum of $\eta(t)$ and $|\breve{\eta}(\omega)|^2$ is the power spectrum corresponding to the signal $\eta(t)$ which is usually denoted by $S(\omega)$.

Besides the autocorrelation, with the probability function we can also define other statistical properties. The nth statistical moment is defined by

$$\mu_n = E[\eta^n] = \int \eta^n f(\eta)d\eta, \tag{2.4}$$

in which f is the probability function for η. In random sea waves, the first statistical moment μ_1 is the mean of the surface elevation. The variance σ^2 is equal to the second central moment,

$$\sigma^2 = \mu_2 = E\left[(\eta-\mu)^2\right] \tag{2.5}$$

σ is also called the standard deviation. The skewness γ and kurtosis κ are defined by

$$\gamma = \frac{\mu_3}{\sigma^3} \tag{2.6}$$

and

$$\kappa = \frac{\mu_4}{\sigma^4} \tag{2.7}$$

The skewness is usually used to estimate the vertical asymmetry of the sea surface elevation, whereas the kurtosis corresponds to the peakedness of the distribution when compared with the normal distribution [14].

A linear superposition of random periodic waves,

$$\eta(x,t) = \sum_n A_n \cos(k_n x - \Omega_n t + \theta_n) \tag{2.8}$$

is a natural representation of sea waves. The amplitudes A_n obey a probability distribution, and the frequencies Ω_n and the wave numbers k_n are related by dispersion relation; the dispersion relation of water waves will be explained in chapter 4. The wave phases θ_n are supposed to be uniformly distributed on the interval $[-\pi, \pi]$. According to [12, 14] the surface wave elevation is described by the Gaussian statistics, so by a distribution defined by:

$$f(\eta) = \frac{1}{\sqrt{2\pi}\sigma} \exp\left[-\frac{(\eta-\mu)^2}{2\sigma^2}\right]$$

Now we consider the unidirectional wave motion of a narrow-band frequency spectrum, for instance using a frequency Ω_m and wave number k_m which correspond to the spectrum peak, then the wave field may be represented in the form

$$\eta(x,t) = |B| \cos(k_m x - \Omega_m t + \varphi) \tag{2.9}$$

where $|B|$ is a slowly varying function of x and t. The distribution of the absolute value of the wave amplitude, $|B|$, and the phase, φ, for a narrow-band process were derived by Massel [14]. The detailed derivation can be seen in Appendix B. The absolute value of the linear wave amplitude is Rayleigh distributed and the phase is uniformly distributed in the range $[-\pi, \pi]$.

$$f_{\text{amp}}(|B|) = \frac{|B|}{\sigma^2} \exp\left(-\frac{|B|^2}{2\sigma^2}\right) \tag{2.10}$$

$$f_{\text{phase}}(\varphi) = \begin{cases} \frac{1}{2\pi} & \text{for } \varphi \in [-\pi, \pi] \\ 0 & \text{for elsewhere} \end{cases} \tag{2.11}$$

Since extreme waves have narrow-band frequency spectrum, the appropriate distribution to estimate the surface wave elevation of extreme waves is the Rayleigh distribution.

2.5 NewWave

As mentioned in section 2.2, the Draupner wave is obviously nonlinear. Walker *et al.* [24] presented a 'design wave' to reproduce the Draupner wave, especially the highest crest. In offshore engineering this design wave has become known as NewWave, which is shown to be an acceptable local model for the linear contribution to large waves [24]. The full model of NewWave is absolutely nonlinear. It is defined using Stokes regular wave expansion up to fifth order, whereas the basis of NewWave is the linear part. It is based on the average shape of an extreme wave in a linear random Gaussian process. The linear NewWave is simply proportional to the auto-correlation function.

Definition Let $S(\omega)$ denote the power spectrum of a given signal $s(t)$. The *linear NewWave* corresponding to the signal $s(t)$ is:

$$\rho(t) = A_N \times \frac{\int S(\omega)\cos(\omega t)d\omega}{\int S(\omega)d\omega} \tag{2.12}$$

where A_N is the magnitude of the maximal amplitude which can be estimated using the Rayleigh distribution and N is the number of waves.

The magnitude of the maximal amplitude, A_N can be computed as long as the probability of the maximal amplitude exceed A_N is defined. On the other hand we can compute the probability of the maximal amplitude if the maximal amplitude, A_N is given. We shall give some illustration of it.

We suppose X to be a random variable which represents the magnitude of the amplitude, then X is Rayleigh distributed with mean μ and variance σ^2. The probability of the maximal amplitude exceed A_N can be denoted as $P(X \geqslant A_N)$. If the maximal amplitude has a return rate 1 in N waves, then its probability is $1/N$. Applying the properties and the definition of distribution function (A.4), we can compute,

$$\begin{aligned} P(X \geqslant A_N) =& 1 - P(X < A_N) = \exp\left(\frac{-A_N^2}{2\sigma^2}\right) \\ A_N =& \sqrt{-2\sigma^2 \ln\left(P(X \geqslant A_N)\right)} \\ =& \sqrt{2\sigma^2 \ln(N)} \end{aligned} \tag{2.13}$$

In the case of the Draupner wave, the maximal amplitude is 18.5[m]. By formula (2.13) the probability of the occurrence of Draupner wave is 4.3E-09 (approximately 1 in 2.3E+08 waves). The total wave height of somewhat less than 26[m] of the extreme waves is estimated to have a return period of 50 years till 100 years (for wave period of 12[s] this is approximately 1 in 1.3E+08 waves till 2.6E+08), but more recent studies based on nonlinear theory, indicate that they may occur more frequently [15]. Therefore the linear theory confirms that the probability of 4.3E-09 is quite realistic to the 100 years wave. In contrast, the amplitude 18.5[m] is absolutely reached by including the nonlinear contribution. The effects of including nonlinear contributions are as one would expect: the crests become narrowed and raised, while the troughs are broadened and raised. Therefore the maximal amplitude of the linear NewWave should be less than 18.5[m]. Walker *et al.* [24] choose a linear NewWave amplitude of 14.7[m], since this corresponds to an amplitude of 18.5[m] in the fifth order NewWave profile, matching the amplitude of the Draupner wave. By choosing the linear NewWave amplitude to be 14.7[m] and substituting the variance of the Draupner signal, $\sigma^2 = 8.88$ in formula 2.13, it can be computed that the probability of the Draupner wave is 5.2E-06, or 1 in 200.000 waves.

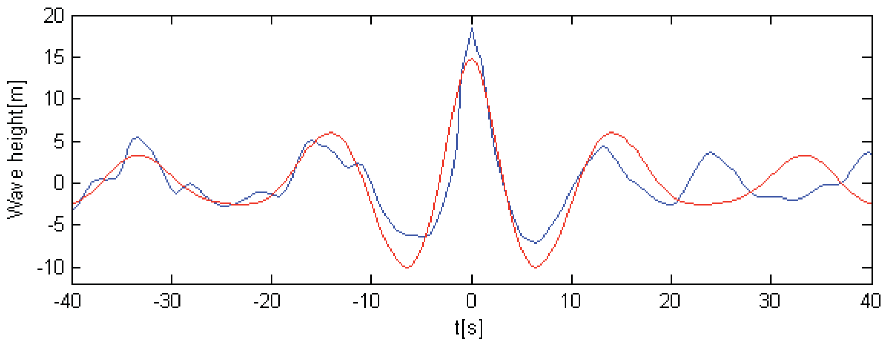

Figure 2.15: The time series of the Draupner wave (blue line) and the time series of linear NewWave (red line) after a time-shift for $N = 200.000$.

$$\begin{aligned} P(X \geqslant A_N) &= \exp\left(\frac{-A_N^2}{2\sigma^2}\right) \\ &= \exp\left(-\frac{14.7^2}{2 \cdot 8.88}\right) \\ &= 5.2\mathrm{E}-06 \end{aligned} \tag{2.14}$$

In other words, the linear amplitude will be 14.7[m] once every 200.000 waves. It is an unlikely occurrence in a record of 100 waves [24], however there are many other records without this extreme crest. Thus, the validity of the probability of the occurrence of extreme crest can be realistic by including many other records.

3

Maximal Wave

3.1 Definition of Maximal Wave

The sea surface elevation at position x and time t will be represented by $\eta(x,t)$. The wave evolution for which the spectrum is given, say $\breve{s}(\omega)$, can be described by

$$\begin{aligned}\eta(x,t) &= \int \breve{s}(\omega) e^{i(k(x-x_0)-\omega t)} d\omega \\ &= \int |\breve{s}(\omega)| e^{i\theta(\omega)} e^{i(k(x-x_0)-\omega t)} d\omega\end{aligned} \tag{3.1}$$

The wave number k, and frequency ω, are related by the dispersion relation $\omega = \Omega(k)$ and $\Omega(k) = -\Omega(-k)$. In principle, Ω can be any skew-symmetric function, $\Omega(k) = -\Omega(-k)$, but in the linear theory of surface waves, Ω is given by (4.2). In the following it is essential that the corresponding evolution is genuine dispersive, i.e that $d^2\Omega/dk^2 \neq 0$ (so we exclude shallow water model for which $\Omega = c_0 k$). We will always restrict to real solution η, so that $\breve{s}(\omega) = \overline{\breve{s}(-\omega)}$, in particular $\theta(\omega) = -\theta(-\omega)$. We aim to introduce a design wave describing an extremal wave evolution, the so-called maximal wave. For any signal we can define the maximal wave with respect to that signal.

Definition Suppose $s(t)$ is a given signal at $x = x_0$ and let $S(\omega)$ be the power spectrum of $s(t)$, $S(\omega) = |\breve{s}(\omega)|^2$. For dispersive evolution, a *maximal wave* corresponding to signal $s(t)$ is the linear wave that is defined as:

$$\eta_{max}(x,t) = \int \sqrt{S(\omega)} e^{i(k(x-x_0)-\omega t)} d\omega \tag{3.2}$$

According to the maximal wave definition, we derive some properties of a maximal wave. We present these properties in Proposition 3.1.1.

Proposition 3.1.1 *Let $\eta(x,t)$ be a wave evolution as described in (3.1). $\eta(x,t)$ is a maximal wave corresponding to signal $s(t)$ if and only if $\eta(x,t)$ satisfies the following conditions*

(1) All phases of the spectrum of signal $s(t)$ are zero

(2) $\eta(x_0,0) = \int \sqrt{S(\omega)}d\omega$ is maximal: $\eta(x_0,0) > \eta(x,t)$ for all $(x,t) \neq (x_0,0)$

(3) By assuming $x_0 = 0$ the symmetry property holds, $\eta(x,t) = \eta(-x,-t)$.

Proof First, suppose η is a maximal wave, then η can be expressed as the form (3.2). Then the η holds the three conditions because:

- The spectrum is real, then the phases are zero

$$\begin{aligned}\eta(x,t) &= \int \breve{s}(\omega)e^{i(k(x-x_0)-\omega t)}d\omega \\ &= \int \sqrt{S(\omega)}e^{i(k(x-x_0)-\omega t)}d\omega \\ \breve{s}(\omega) &= \sqrt{S(\omega)} \in \mathbb{R}\end{aligned}$$

- Substituting $(x_0,0)$ in (3.2) gives $\eta(x_0,0) = \int \sqrt{S(\omega)}d\omega$ which is clearly a maximal

- Substituting $x_0 = 0$ gives

$$\begin{aligned}\eta(x,t) &= \int \sqrt{S(\omega)}e^{i(K(\omega)x-\omega t)}d\omega \\ &= \int \sqrt{S(-\varphi)}e^{i(K(-\varphi)x+\varphi t)}d\varphi \\ &= \int \sqrt{S(\varphi)}e^{i(K(\varphi).(-x)-\varphi(-t))}d\varphi \\ &= \eta(-x,-t)\end{aligned}$$

  since the dispersion relation is skew-symmetric, $K(-\varphi) = -K(\varphi)$.

On the other hand, suppose that the three conditions are satisfied and that η is given by (3.1). From *(1)* it follows $\theta(\omega) \equiv 0$, hence

$$\eta(x,t) = \int |\breve{s}(\omega)|e^{i(k(x-x_0)-\omega t)}d\omega$$

Condition *(2)* gives $\breve{s}(\omega) = \sqrt{S(\omega)}$, while the symmetric property in *(3)* gives the skew-symmetric of the dispersion relation. Consequently the η is a maximal wave and can be expressed by

$$\eta(x,t) = \int \sqrt{S(\omega)}e^{i(k(x-x_0)-\omega t)}d\omega = \quad \eta_{max}(x,t)$$

3.2 Irregular Wave

The ocean surface is often a combination of many wave components. Consequently, most of the wave surface are 'irregular', which is by definition (modelled) as a wave with random phases:

Definition For given a power spectrum $S(\omega)$, the corresponding irregular wave is defined by:

$$\eta_{irr}(x,t) = \int \sqrt{S(\omega)} e^{i\theta(\omega)} e^{i(kx-\omega t)} d\omega \tag{3.3}$$

where $\theta(\omega)$ is a random number in the range $[-\pi, \pi]$.

3.3 Pseudo-Maximal Wave

3.3.1 Definition of Pseudo-Maximal Wave

As investigated in section 2.3, the phases of the full time series Draupner signal are random in the range $[\pi, \pi]$ with mean zero and deviation 0.56π. This seems to be an irregular wave. On the other hand the phases of the Draupner signal around highest wave we are interested in are no longer random, so this can not be an irregular wave. In the definition of maximal wave there is a restriction that the phases are zero, so the Draupner wave can not be a maximal wave. Consequently, the Draupner wave is neither an irregular nor a maximal wave. That motivates us to introduce a new design wave that seems to be in between irregular and maximal wave, so-called pseudo-maximal wave. The phases of this design wave are random in a restricted phase interval. We denote $\theta_a \in U(-a\pi, a\pi)$ as the random phases restricted in $(-a\pi, a\pi)$.

Definition Let a be a number in $(0,1)$. Suppose $s(t)$ is a given signal at $x = x_0$ and $\theta_a(\omega)$ is a random number in $(-a\pi, a\pi)$. A *pseudo-maximal wave* (PMW) corresponding to a and signal $s(t)$ is the linear wave which is defined as :

$$\eta_{pmw(a)}(x,t) = \underset{\theta_a \in U(-a\pi, a\pi)}{\text{Average}} \left[\int \sqrt{S(\omega)} e^{i\theta_a(\omega)} e^{i(k(x-x_0)-\omega t)} d\omega \right] \tag{3.4}$$

where $S(\omega)$ is the power spectrum of $s(t)$.

It is obvious that the first property of a maximal wave is no longer satisfied by PMW because of the random phases of θ_a. However we will show that PMW satisfies the symmetry property of a maximal wave. It can be investigated by analyzing the distribution of PMW. An important property of PMW is the restriction of the random phases in the range $(-a\pi, a\pi)$, so that the PMW also depends on a. It is interesting to know the effect of the value of a to the PMW. We will investigate that in section 3.3.3.

3.3.2 Distribution of $\sin(\theta_a(\omega))$ and $\cos(\theta_a(\omega))$

Basically the PMW is the average of all waves with the same power spectrum but with phases taken from $U(-a\pi, a\pi)$. Before studying the distribution of PMW, it is essential to study the distribution of PMW at the maximal point, i.e at $(x_0, 0)$. From equation (3.4) we can obtain the PMW at $x = x_0$ and $t = 0$,

$$\eta_{pmw(a)}(x_0, 0) = \underset{\theta_a \in U(-a\pi, a\pi)}{\text{Average}} \left[\int \sqrt{S(\omega)} e^{i\theta_a(\omega)} d\omega \right] \tag{3.5}$$

Initially we should study the distribution of $e^{i\theta_a(\omega)}$. To simplify notation, we write θ_a. Since $e^{i\theta_a} = \cos(\theta_a) + i\sin(\theta_a)$, we need to investigate the distribution of $\sin(\theta_a)$ and $\cos(\theta_a)$.

Let $\theta_a \sim U(-a\pi, a\pi)$. Denote the distribution function of θ_a by $F_{\theta_a}(x)$, then

$$F_{\theta_a}(x) = P(\theta_a \leqslant x) = \begin{cases} 0 & \text{for } x < -a\pi \\ \frac{x+a\pi}{2a\pi} & \text{for } -a\pi \leqslant x < a\pi \\ 1 & \text{for } x \geqslant a\pi \end{cases} \tag{3.6}$$

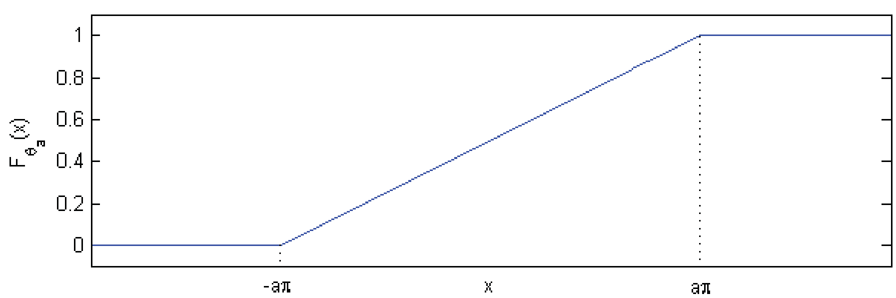

Figure 3.1: Distribution function of the phases, $\theta_a \sim U(-a\pi, a\pi)$

First, we look into the distribution of $\sin(\theta_a)$. Let $Y = g(\theta_a) = \sin(\theta_a)$, then Y is also a random variable since, for any outcome y, $Y(y) = \sin(\theta_a(y))$. It is not simple to define the distribution of Y since the $\sin^{-1}$ is only defined on $[-\frac{\pi}{2}, \frac{\pi}{2}]$. Consequently we separate the distribution of $\sin(\theta_a)$ in two cases, for $a \in (0, 1/2]$ and for $a \in (1/2, 1)$. In the case $a \in (0, 1/2]$ see Figure 3.2, we can compute the distribution function of Y, $F_Y(y)$ or $F_{\sin(\theta_a)}(y)$ easily as:

$$
\begin{aligned}
F_{\sin(\theta_a)}(y) =& P(\sin(\theta_a) \leqslant y) \\
=& P(-a\pi \leqslant \theta_a \leqslant \sin^{-1}(y)) \\
=& F_{\theta_a}(\sin^{-1}(y)) - F_{\theta_a}(-a\pi) \\
=& F_{\theta_a}(\sin^{-1}(y)) \\
=& \begin{cases} 0 & \text{for } y < \sin(-a\pi) \\ \frac{\sin^{-1}(y)+a\pi}{2a\pi} & \text{for } \sin(-a\pi) \leqslant y < \sin(a\pi) \\ 1 & \text{for } y \geqslant \sin(a\pi) \end{cases}
\end{aligned}
$$

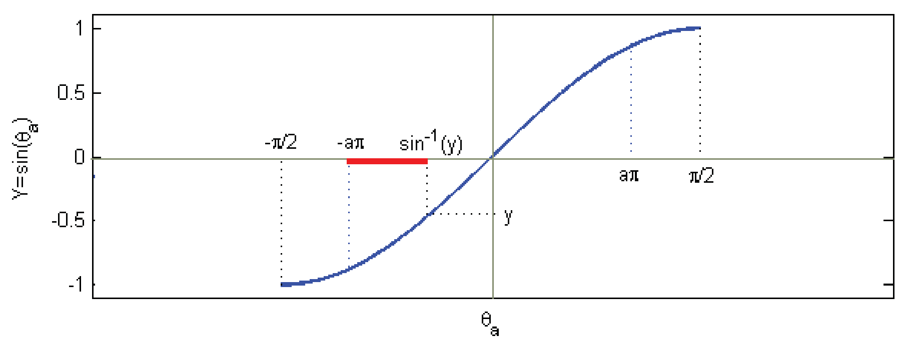

Figure 3.2: Sketch for computing $F_{\sin(\theta_a)}(y)$ with $a \in (0, 1/2]$

On the other hand, we may compute the distribution function of Y, $F_Y(y)$ or $F_{\sin(\theta_a)}(y)$ for $a \in (1/2, 1)$ (see Appendix C) and we obtain

$$
F_{\sin(\theta_a)}(y) = \begin{cases} 0 & \text{for } y < -1 \\ \frac{\sin^{-1}(y)}{a\pi} + \frac{1}{2a} & \text{for } -1 \leqslant y < \sin(-a\pi) \\ \frac{\sin^{-1}(y)}{2a\pi} + \frac{1}{2} & \text{for } \sin(-a\pi) \leqslant y < \sin(a\pi) \\ 1 + \frac{\sin^{-1}(y)}{a\pi} - \frac{1}{2a} & \text{for } \sin(a\pi) \leqslant y < 1 \\ 1 & \text{for } y \geqslant 1 \end{cases}
$$

Second, by the same way we derive the distribution function of $\cos(\theta_a)$. This is much simpler since cosine is an even function. We consider that $\cos^{-1}$ is defined in $[0, \pi]$.

From Figure 3.3 we can compute the distribution function of $\cos(\theta_a)$ easily as:

$$
\begin{aligned}
F_{\cos(\theta_a)}(y) =& P(\cos(\theta_a) \leqslant y) \\
=& 2P\left(\cos^{-1}(y) \leqslant \theta_a \leqslant a\pi\right) \\
=& 2\left[F_{\theta_a}(a\pi) - F_{\theta_a}\left(\cos^{-1}(y)\right)\right] \\
=& 2\left[1 - F_{\theta_a}(\cos^{-1}(y))\right] \\
=& \begin{cases} 0 & \text{for } y < \cos(a\pi) \\ 1 - \frac{\cos^{-1}(y)}{a\pi} & \text{for } \cos(a\pi) \leqslant y < 1 \\ 1 & \text{for } y \geqslant 1 \end{cases}
\end{aligned}
\tag{3.7}
$$

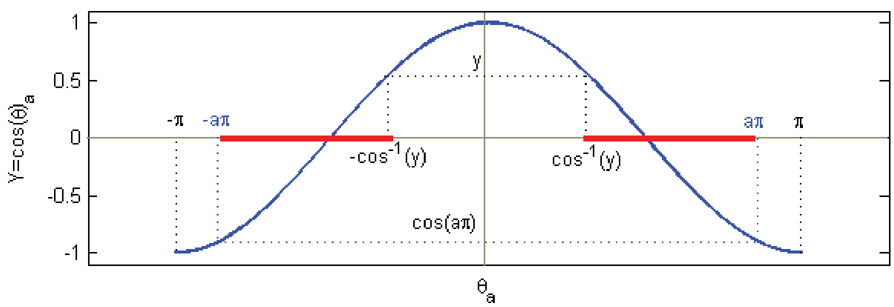

Figure 3.3: Sketch for computing $F_{\cos(\theta_a)}(y)$ with $a \in (0, 1)$

The probability functions of these distributions are:

$$
f_{\sin(\theta_a)}(y) = \frac{dF_{\sin(\theta_a)}(y)}{dy} = \begin{cases} 0 & \text{for } y < \sin(-a\pi) \text{ or } y \geqslant \sin(a\pi) \text{ and } a \in (0, 1/2] \\ \frac{1}{2a\pi\sqrt{1-y^2}} & \text{for } \sin(-a\pi) \leqslant y < \sin(a\pi) \text{ and } a \in (0, 1/2] \end{cases}
$$

$$
f_{\sin(\theta_a)}(y) = \frac{dF_{\sin(\theta_a)}(y)}{dy} = \begin{cases} 0 & \text{for } y < -1 \text{ or } y \geqslant 1 \text{ and } a \in (1/2, 1) \\ \frac{1}{a\pi\sqrt{1-y^2}} & \text{for } -1 < y \leqslant \sin(-a\pi) \text{ or } \sin(a\pi) < y \leqslant 1 \\ & \text{and } a \in (1/2, 1) \\ \frac{1}{2a\pi\sqrt{1-y^2}} & \text{for } \sin(-a\pi) \leqslant y < \sin(a\pi) \text{ and } a \in (1/2, 1) \end{cases}
$$

$$
f_{\cos(\theta_a)}(y) = \frac{dF_{\cos(\theta_a)}(y)}{dy} = \begin{cases} 0 & \text{for } y < \cos(a\pi) \text{ or } y \geqslant 1 \text{ and } a \in (0, 1) \\ \frac{1}{a\pi\sqrt{1-y^2}} & \text{for } \cos(a\pi) \leqslant y < 1 \text{ and } a \in (0, 1) \end{cases}
$$

Applying the defined probability function above to the mean and variance definition, we can compute the mean (μ) and the variance (σ^2) of these distributions. For instance, the mean of $Y = \cos(\theta_a)$ is computed by:

$$\begin{aligned}\mu = E[Y] = E[\cos(\theta_a)] &= \int_{\cos(a\pi)}^{1} y \cdot f_{\cos(\theta_a)}(y)dy \\ &= \int_{\cos(a\pi)}^{1} y \cdot \frac{1}{a\pi\sqrt{1-y^2}}dy \\ &= \frac{1}{a\pi}\sqrt{1-\cos^2(a\pi)}\end{aligned} \tag{3.8}$$

while the variance of $Y = \cos(\theta_a)$ is:

$$\begin{aligned}\mathrm{Var}(Y) = \sigma^2 &= E[Y^2] - E[Y]^2 \\ E[Y^2] &= \int_{\cos(a\pi)}^{1} y^2 \cdot f_{\cos(\theta_a)}(y)dy \\ &= \int_{\cos(a\pi)}^{1} y^2 \cdot \frac{1}{a\pi\sqrt{1-y^2}}dy \\ &= \frac{1}{2a\pi}\left[a\pi + \cos(a\pi)\sqrt{1-\cos^2(a\pi)}\right] \\ \mathrm{Var}(Y) = \mathrm{Var}(\cos(\theta_a)) &= \frac{1}{2a\pi}\left[a\pi + \cos(a\pi)\sqrt{1-\cos^2(a\pi)}\right] - \frac{1}{a^2\pi^2}\left[1-\cos^2(a\pi)\right]\end{aligned} \tag{3.9}$$

For example $\theta \sim U(-\frac{\pi}{2}, \frac{\pi}{2})$. The distribution of $\sin(\theta)$ is (see Figure 3.4):

$$\begin{aligned}F_{\sin(\theta_{.5})}(y) &= \begin{cases} 0 & \text{for } y < -1 \\ \frac{\sin^{-1}(y)}{\pi} + \frac{1}{2} & \text{for } -1 \leqslant y < 1 \\ 1 & \text{for } y \geqslant 1 \end{cases} \\ f_{\sin(\theta_{.5})}(y) &= \begin{cases} 0 & \text{for } y \leqslant -1 \text{ or } y \geqslant 1 \\ \frac{1}{\pi\sqrt{1-y^2}} & \text{for } -1 < y < 1 \end{cases}\end{aligned} \tag{3.10}$$

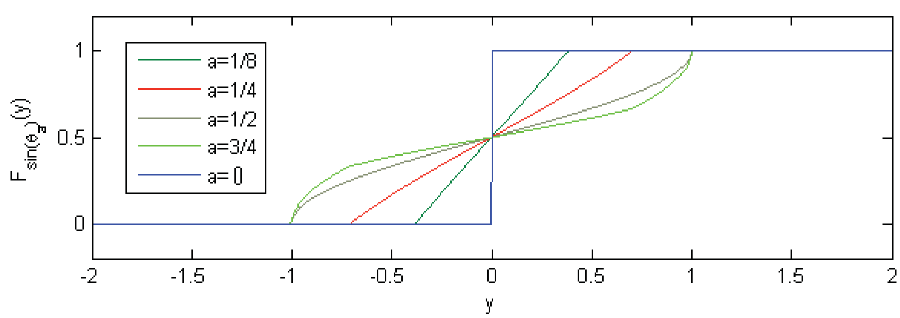

Figure 3.4: Distribution function of $Y = \sin(\theta)$, where $\theta \sim U(-a\pi, a\pi)$

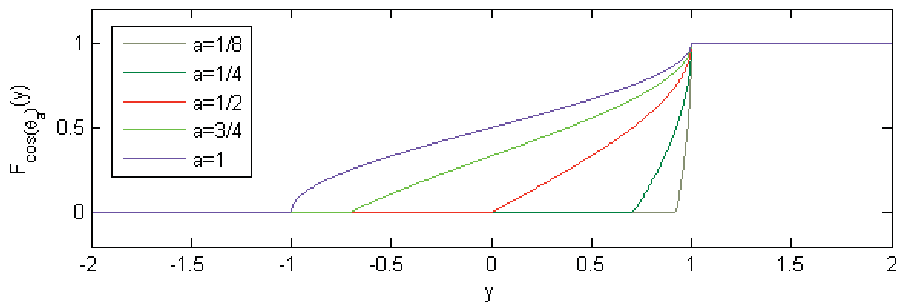

Figure 3.5: Distribution function of $Y = \cos(\theta)$, where $\theta \sim U(-a\pi, a\pi)$

The distribution of $\cos(\theta)$ for which $\theta \sim U(-\frac{\pi}{2}, \frac{\pi}{2})$ is (See Figure 3.5):

$$F_{\cos(\theta_{.5})}(y) = \begin{cases} 0 & \text{for } y < 0 \\ 1 - \frac{2\cos^{-1}(y)}{\pi} & \text{for } 0 \leqslant y < 1 \\ 1 & \text{for } y \geqslant 1 \end{cases}$$

$$f_{\cos(\theta_{.5})}(y) = \begin{cases} 0 & \text{for } y \leqslant 0 \text{ or } y \geqslant 1 \\ \frac{2}{\pi\sqrt{1-y^2}} & \text{for } 0 < y < 1 \end{cases}$$

3.3.3 Distribution of PMW

PMW is obviously a function of x, t, and a. As investigated in previous section we first analyze the distribution of PMW at $(x_0, 0)$, so that PMW will be only a function of a as described in (3.5). By describing the distribution of $\eta_{pmw(a)}(x_0, 0)$ corresponding to the value of a we can study the effect of the phases on the PMW. Further we describe the distribution of PMW for any (x, t) which can be used to investigate the symmetry property of PMW.

As mentioned before the PMW is the average of a random variable, let Z_a be the random variable, then we may define Z_a as:

$$Z_a = \int \sqrt{S(\omega)} e^{i\theta_a(\omega)} d\omega \text{ for } a \in (0, 1) \tag{3.11}$$

Analytically we compute the average of a random variable by its expected value. In probability theory, by the strong law of large numbers (SLLN) theorem we describe the result of performing the same experiment a large number of times. According to the law, the average of the results obtained from a large number of trials should be close to the expected value, and will tend to become closer as more trials are performed. Therefore, we can write the PMW (3.5) by:

$$\underset{\theta_a \in U(-a\pi, a\pi)}{\text{Average}} \left[\int \sqrt{S(\omega)} e^{i\theta_a(\omega)} d\omega \right] = \underset{\theta_a \in U(-a\pi, a\pi)}{\text{Average}} [Z_a] = E[Z_a]$$

Theorem 3.3.1 ***(Strong Law of Large Numbers)*** *If $X_1, X_2, \ldots$ are independent and identically distributed with mean μ, then*

$$P\left\{ \lim_{n\to\infty} \left(\frac{X_1 + \ldots + X_n}{n} \right) = \mu \right\} = 1$$

Theorem 3.3.2 ***(Central Limit Theorem)*** *If $X_1, X_2, \ldots$ are independent and identically distributed with mean μ and variance σ^2, then*

$$\lim_{n\to\infty} P\left\{ \frac{X_1 + \ldots + X_n - n\mu}{\sigma\sqrt{n}} \leqslant a \right\} = \int_{-\infty}^{a} \frac{1}{\sqrt{2\pi}} e^{-x^2/2} dx$$

Thus, if we let $S_n = \sum_{i=1}^{n} X_i$, where $X_1, X_2, \ldots$ are i.i.d, then the Central Limit Theorem (CLT) states that S_n has a normal distribution as $n \to \infty$ [20].

Before computing the expected value of Z_a, we observe the distribution of Z_a. We express $A(\omega_k) = \sqrt{S(\omega_k)}\Delta\omega_k$, so we may define the integral form of Z_a restricted to the real value by a Riemann sum as:

$$\begin{aligned} Z_a &= \lim_{K\to\infty} \sum_{k=1}^{K} \sqrt{S(\omega_k)} \cos(\theta_a(\omega_k)) \Delta(\omega_k) \\ &= \lim_{K\to\infty} \sum_{k=1}^{K} A(\omega_k) \cos(\theta_a(\omega_k)) \end{aligned} \tag{3.12}$$

Applying the CLT for i.i.d random variables, $A(\omega_k)\cos(\theta_a(\omega_k))$, we conclude that Z_a has a normal distribution. The expected value of Z_a can be computed by:

$$\begin{aligned} \mu_a = E[Z_a] =& E\left[\lim_{K\to\infty} \sum_{k=1}^{K} A(\omega_k) \cos(\theta_a(\omega_k)) \right] \\ =& E\left[\cos(\theta_a(\omega_k))\right] \lim_{K\to\infty} \sum_{k=1}^{K} A(\omega_k) \\ =& E\left[\cos(\theta_a)\right] \int \sqrt{S(\omega)} d\omega \end{aligned}$$

By substituting (3.8) into the equation above, we obtain the mean of Z_a as a function of a.

$$\mu_a = E[Z_a] = \frac{1}{a\pi}\sqrt{1-\cos^2(a\pi)}\int\sqrt{S(\omega)}d\omega \tag{3.13}$$

Figure 3.6 shows the mean of Z_a and also the deviation of Z_a measured from the mean. Meanwhile the variance of Z_a, $\mathrm{Var}(Z_a)$, can be computed by:

$$\begin{aligned}
\mathrm{Var}(Z_a) =& \mathrm{Var}\left(\lim_{K\to\infty}\sum_{k=1}^{K} A(\omega_k)\cos(\theta_a(\omega_k))\right)\\
=& \lim_{K\to\infty}\mathrm{Var}\left(\sum_{k=1}^{K} A(\omega_k)\cos(\theta_a(\omega_k))\right)\\
=& \mathrm{Var}(\cos(\theta_a))\lim_{K\to\infty}\sum_{k=1}^{K}\left(A(\omega_k)\right)^2\\
=& \left(\frac{1}{2a\pi}\left[a\pi+\cos(a\pi)\sqrt{1-\cos^2(a\pi)}\right]-\frac{1}{a^2\pi^2}\left[1-\cos^2(a\pi)\right]\right)\lim_{K\to\infty}\sum_{k=1}^{K}\left(A(\omega_k)\right)^2
\end{aligned} \tag{3.14}$$

and it is shown in Figure 3.7 under assumption $\lim_{K\to\infty}\sum_{k=1}^{K}\left(A(\omega_k)\right)^2 = 1$.

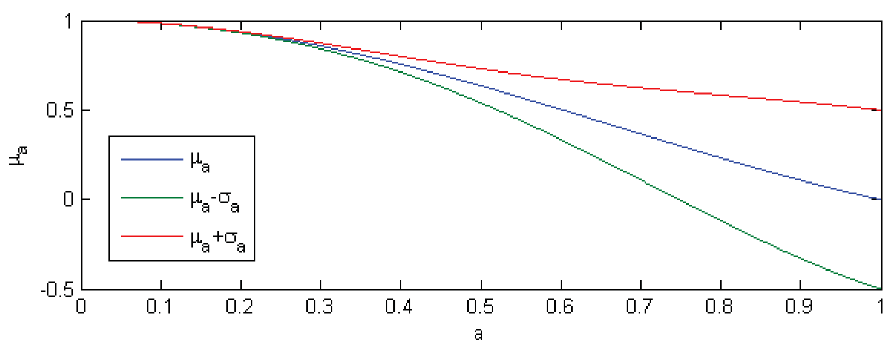

Figure 3.6: Expected value of PMW and deviation with standard deviation at $(x_0, 0)$ as a function of a with $\int\sqrt{S(\omega)}d\omega = 1$

All results in this section can be summarized by saying that the PMW at $(x_0, 0)$ corresponding to a is normally distributed and it converges to $E[Z_a]$. Additionally we can illustrate the effect of the phases to the maximum value of PMW in Figure 3.6. The PMW at $(x_0, 0)$ decreases as the range of the phases is getting narrower. For $a = 1$, the phases are in $(-\pi, \pi)$ and the expected value of PMW are zero.

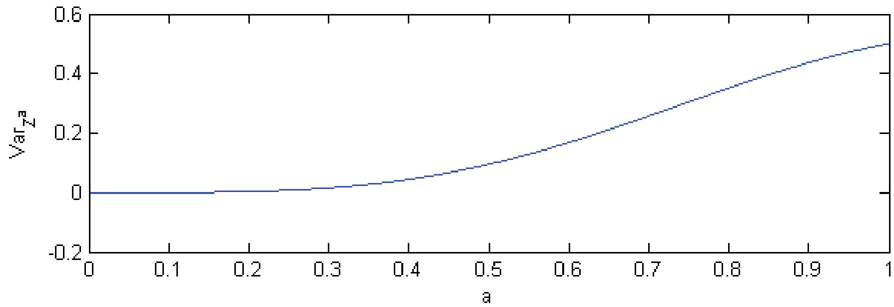

Figure 3.7: Variance of PMW at $(x_0, 0)$ as a function of a

In fact the time t and the space x do not change the distribution of PMW. The PMW at (x, t) corresponding to a is still normally distributed for all (x, t). The derivation can be executed in the same way as derivation of the distribution of PMW at $(x_0, 0)$ by including $e^{i(k(x-x_0)-\omega t)}$ in the integral. The difference is only the parameter distribution, the mean and the variance. As the generalization of (3.13), the PMW at (x, t) will converge to $\mu_a(x, t)$. Since we have proved that a maximal wave is symmetric, then $\mu_a(x, t)$ will be symmetric as well. This is shown in equation below:

$$\begin{aligned}
\mu_a(x,t) =& \frac{1}{a\pi}\sqrt{1-\cos^2(a\pi)} \int \sqrt{S(\omega)} e^{i(k(x-x_0)-\omega t)} d\omega \\
=& \frac{1}{a\pi}\sqrt{1-\cos^2(a\pi)} \eta_{max}(x,t) \\
=& \frac{1}{a\pi}\sqrt{1-\cos^2(a\pi)} \eta_{max}(-x,-t) \\
=& \mu_a(-x,-t)
\end{aligned} \tag{3.15}$$

Finally we conclude that the PMW corresponding to any a holds the symmetry property of a maximal wave.

3.4 Comparing the Draupner wave with (Pseudo-) Maximal Draupner Wave

3.4.1 Maximal Draupner Wave

By the definition of a maximal wave, the maximal Draupner wave at $(0, t)$ can be expressed as:

$$\eta_{max}(t) = \eta(0,t) = \int \sqrt{S(\omega)} e^{-i\omega t} d\omega \tag{3.16}$$

where $S(\omega) = |\breve{\eta}(x_0, \omega)|^2$ is the power spectrum of the time signal $s(t)$. For the Draupner signal as given in Figure 2.10, we get the corresponding maximal wave (maximal Draupner wave), $\eta_{max}(t)$ as plotted in Figure 3.8.

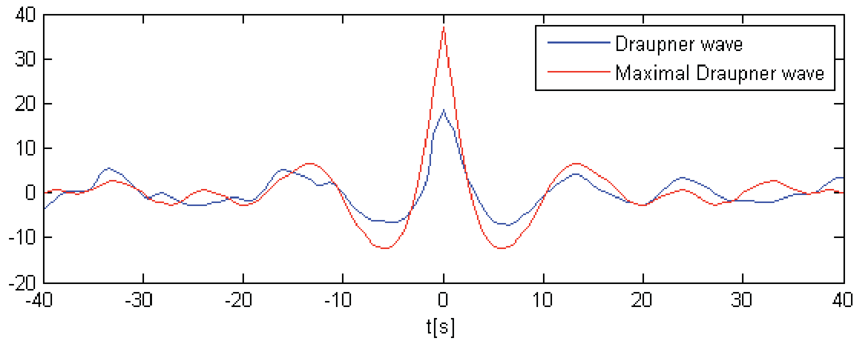

Figure 3.8: The Draupner signal and the corresponding maximal wave

There is a very large differences around $t = 0$ if we compare the maximal Draupner wave and the Draupner wave itself. The maximal amplitude of the Draupner wave is 18.5[m], but the maximal amplitude of the maximal Draupner wave is about 37.25[m], about two times larger. The reason must be because a maximal wave is valid for a wave which has zero phases, while the Draupner wave has dominantly phases in $(-0.61\pi, 0.61\pi)$. Due to the fact that the maximal Draupner wave can not model the maximal crest of the Draupner wave, we use PMW as the extension of the maximal wave which will indeed decrease the maximal amplitude.

3.4.2 Pseudo Maximal Draupner wave

For the Draupner wave in the interval as used in section 2.3 we define the PMW corresponding to that, so-called pseudo-maximal Draupner wave (PMDW), as:

$$\eta_{pmw(a)}(t) = \underset{\theta_a \in U(-a\pi, a\pi)}{\text{Average}} \left[\int \sqrt{S(\omega)} e^{i\theta_a(\omega)} e^{-i\omega t} d\omega \right] \tag{3.17}$$

We are interested in the maximal amplitude. To that end, we performed simulations to calculate the average, and compare with analytic results. For the simulation we choose $N = 1000$, i.e we take the average of 1000 trials for $\theta(\omega)$. For $t = 0$ we obtain $\eta_{pmw(a)}(0)$ as shown in Figure 3.9 for discrete value of a. As N increases $\eta_{pmw(a)}(0)$

will converge to a function that we have derived before, that is (3.13). We call it the analytic mean of PMW and the graph is also plotted in Figure 3.13. Observe that for $N = 1000$ the simulation results are very close to the analytic result.

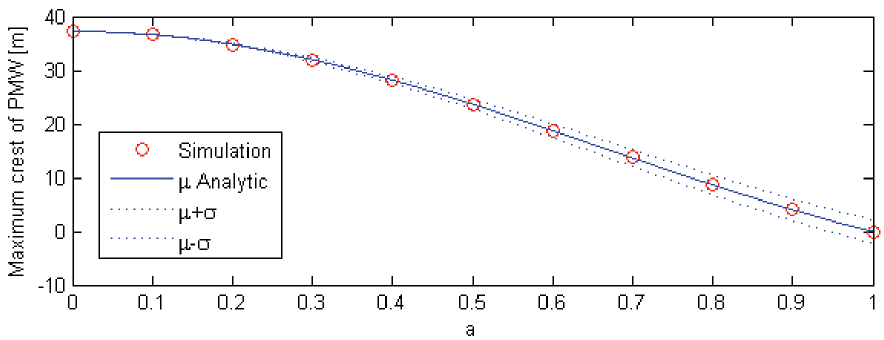

Figure 3.9: Maximal crest height of PMDW (circle red) obtained by simulation, and the analytic value of the crest height of PMDW (blue line)

Our aim is to find the PMDW which can approximate the Draupner wave well around the maximal amplitude. The maximal amplitude of the Draupner wave is 18.5[m], so we want to find the appropriate value of a such that $\eta_{pmw(a)}(0)$ is exactly 18.5[m]. Analytically we can estimate the appropriate value of a by applying the Draupner signal and substituting 18.5 into μ_a in the equation (3.13). The appropriate value of a is 0.606, the solution of the equation below:

$$18.5 = \frac{1}{a\pi}\sqrt{1-\cos^2(a\pi)}\int\sqrt{S(\omega)}d\omega$$

On the other hand we can also get the value of a from the simulation result as shown in Figure 3.9. The zoomed figure is in Figure 3.10. From this figure the desired crest height is indeed found at $a = 0.606$. Actually we can also find the desired crest height 18.5[m] in the range $a \in (0.58; 0.64)$ within one standard deviation. According to [24], the amplitude of 18.5[m] is obtained with the nonlinear contribution, whereas the linear contribution of the Draupner wave has a maximal amplitude of 14.7[m]. Consequently the value of a corresponding to the linear amplitude is 0.68 or in the range $(0.65; 0.71)$ within one standard deviation.

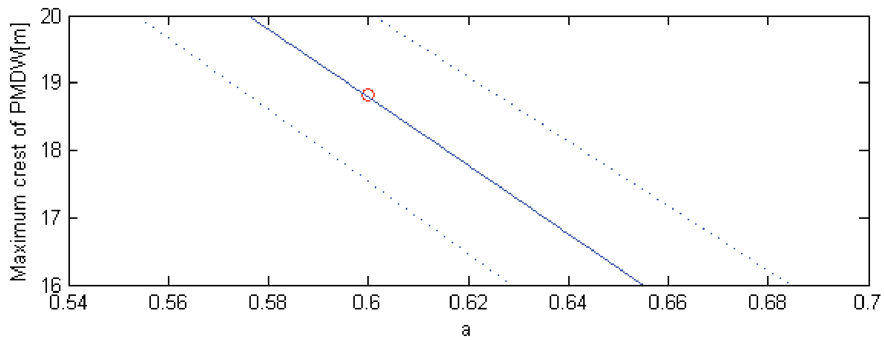

Figure 3.10: A closer look of maximal crest height 18.5[m]

In addition we calculate the height of PMDW as function of a at other times t, see Figure 3.11. The graph of PMDW at time t is precisely the same as at time $-t$. Figure 3.11 shows that the maximal of PMDW is at $t = 0$.

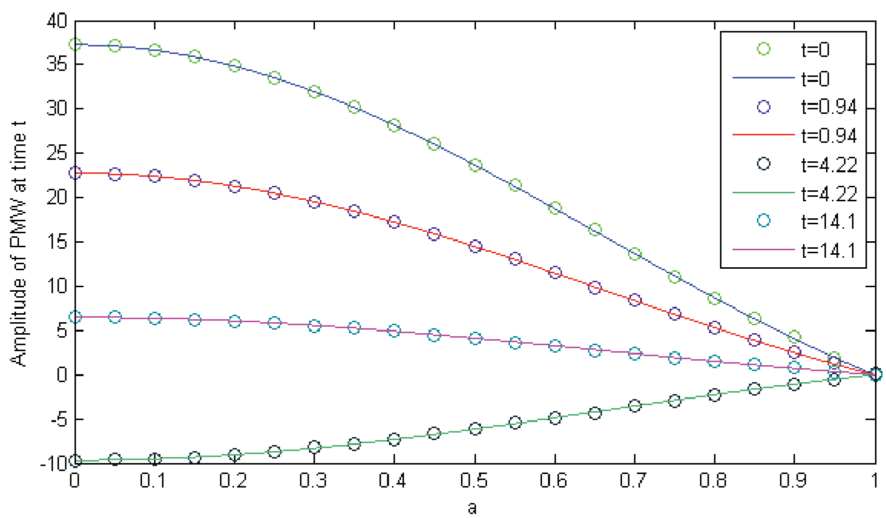

Figure 3.11: Amplitude of PMDW (circle) obtained by simulation, and the analytic mean of PMDW at certain t (solid line)

From Figure 3.9 we see that the maximal crest height is getting lower as a increases. The effect of changing the phases can also be seen directly in Figure 3.12 till Figure 3.16. These figures are the PMDW corresponding to various value for a.

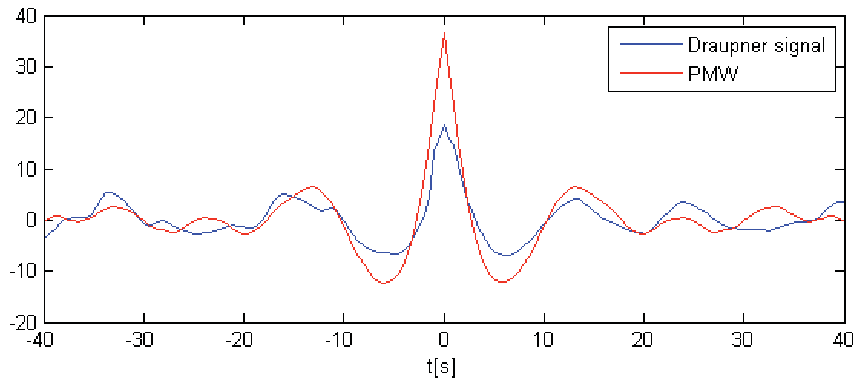

Figure 3.12: The Draupner signal and PMDW with $a = 0.1$

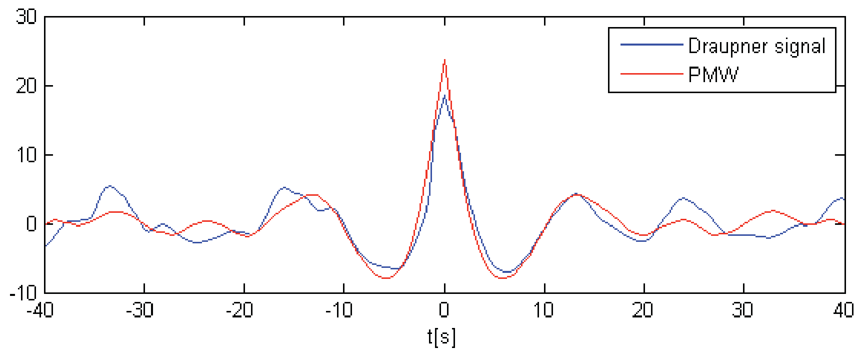

Figure 3.13: The Draupner signal and PMDW with $a = 0.5$

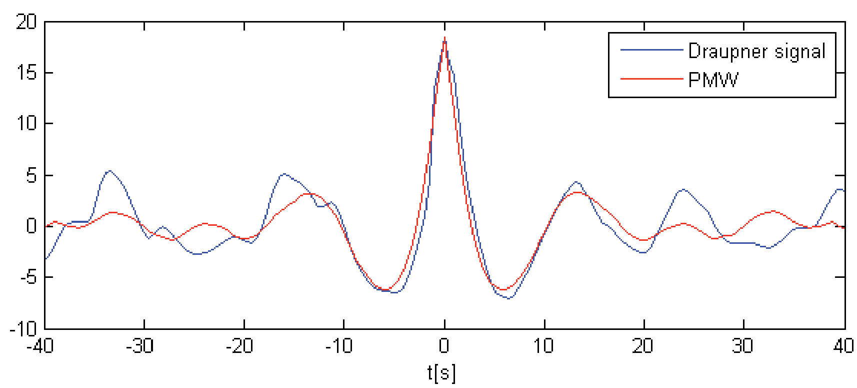

Figure 3.14: The Draupner signal and PMDW with $a = 0.606$

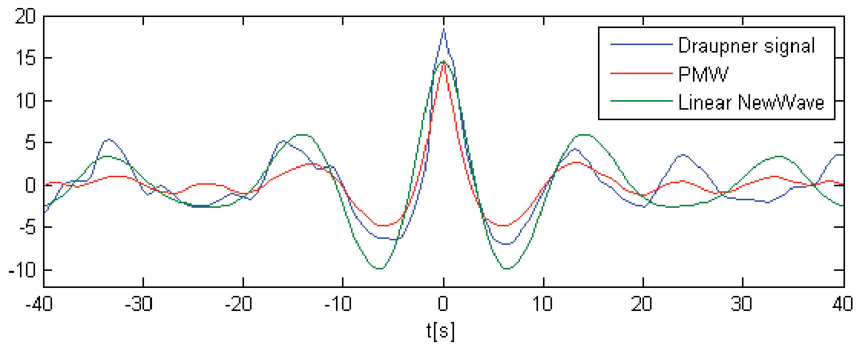

Figure 3.15: The Draupner signal, PMDW with $a = 0.68$, and the linear NewWave

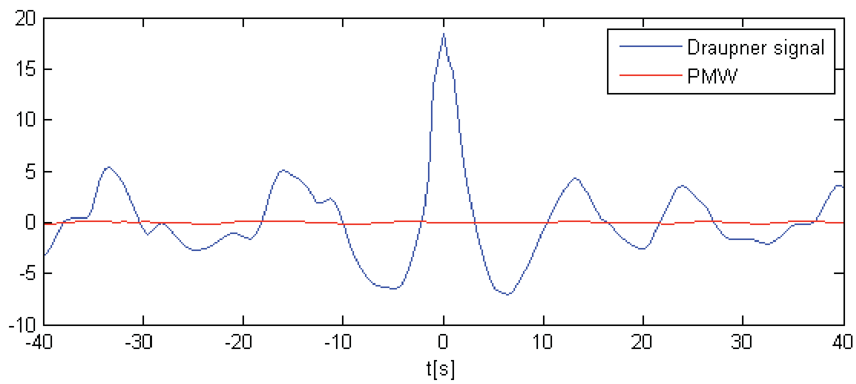

Figure 3.16: The Draupner signal and PMDW with $a = 1$

These figures show the effect of restriction of the phases. The maximal crest height decreases rapidly and the symmetry property is obviously satisfied by PMDW which is shown in formula (3.15). For $a = 0$ we obtain the maximal wave and for $a = 1$ we get the mean of N irregular wave, which is zero. We observe from Figure 3.12 that for $a = 0.1$ the maximal crest height is still very high, whereas Figure 3.16 shows that for $a = 1$ there is almost nothing. The PMDW in Figure 3.14 has maximal crest height 18.5[m], since $a = 0.606$ is the appropriate value to reproduce the maximal crest height of the Draupner wave. It is not only good for approximating the maximal crest height, but the PMDW corresponding to $a = 0.606$ is also quite good to model the Draupner wave in an interval near crest $t \in (-10, 10)$.

We are now interested in Figure 3.15, which shows the linear contribution of the Draupner wave. The maximal amplitude of the linear NewWave is 14.7[m] [24]. The PMDW with $a = 0.68$ also has maximal amplitude of 14.7[m]. By comparing the graphs plotted in Figure 3.15 we observe that: 1) the crest of PMDW is narrower than the crest of the linear NewWave, while the trough is broader and higher; 2) the trough of PMDW is also broader and higher than the trough of the Draupner wave; 3) the crest of the linear NewWave is wider than the crest of the Draupner wave, while the trough is broader and lower.

4

Spatial Evolution of the Draupner Wave using AB equation

This chapter describes the spatial evolution of the Draupner wave with the AB equation. It also demonstrates how well Draupner wave satisfies the symmetry property. We perform simulations of the wave evolution as a signaling problem for the linear and the nonlinear AB equation. A signaling problem is a problem for a wave model that specifies the surface elevation at one position as a function of time and aims to calculate the wave elevation at every position and every time. We will take the Draupner signal to specify the elevation at the Draupner position.

4.1 AB equation

The AB equation derived by van Groesen and Andonowati [22] is a unidirectional wave equation above a flat bottom describing the surface wave elevation. This equation is derived by exploiting the variational formulation of surface water wave [22]. It is applicable for finite and infinite depth, but in this study we use only the equation for finite depth. We describe the dynamics by the surface elevation, $\eta(x,t)$. As defined in [22], the AB equation can be written as:

$$\partial_t \eta = \pm\sqrt{g}A\left[\eta + \frac{1}{4}(B\eta)^2 + \frac{1}{2}B(\eta B\eta) - \frac{1}{4}(A\eta)^2 + \frac{1}{2}A(\eta A\eta)\right] \tag{4.1}$$

where A and B are the pseudo differential operators which depend on the dispersion relation (see also [23]). The equation (4.1) is the nonlinear AB equation, while the linear AB equation is only the first term in square brackets. The minus sign in equation (4.1) is for the wave evolution travelling to the right and the plus sign is for the wave evolution travelling to the left. Since we consider dispersive wave evolution, we need the dispersion relation for water waves. According to Whitham [26], in one space dimension, water waves on a layer of depth h in a constant gravity field g, have dispersion given by the relation,

$$\omega = \Omega(k) = \mathrm{sign}(k)\sqrt{gk\tanh(kh)} \tag{4.2}$$

where k is the wave number. The operators A and B are defined by:

$$A = C\frac{\partial_x}{\sqrt{g}} \qquad B = \frac{\sqrt{g}}{C} \tag{4.3}$$

in which C is the phase velocity operator. The Fourier transfrom of C is defined by $\widehat{C} = \frac{\Omega(k)}{k}$, therefore we can derive the Fourier transform of operator A as:

$$\widehat{A} = i\ \mathrm{sign}(k)\sqrt{k\tanh(kh)} = \frac{i\Omega(k)}{\sqrt{g}} \tag{4.4}$$

and the Fourier transform of operator B as:

$$\widehat{B} = \sqrt{\frac{k}{\tanh kh}} \tag{4.5}$$

The idea to solve the AB equation is by transforming the equation into Fourier space, as shown in section 4.2 and 4.3 in more detail.

4.2 The Signaling problem for Dispersive AB equation

The aim of this section is to define the signaling problem that we will use in the numerical simulation. There will be two cases, the signaling problem for linear dispersive AB equation and the signaling problem for nonlinear dispersive AB equation. In the simulation we use the Draupner signal in small interval as described in section 2.3 as the signal to be generated at $x = 0$, $s(t)$.

Firstly, we formulate the signaling problem for the linear dispersive AB equation as:

$$\begin{aligned} \partial_t\eta =& \pm\sqrt{g}A\eta \\ \eta(0,t) =& s(t) \end{aligned} \tag{4.6}$$

By solving (4.6) we obtain the signals at other places in the domain. By investigating $\eta(x,t)$ and $\eta(-x,-t)$, we can observe how good the simulation satisfy the symmetry property.

As mentioned before we want to solve the problem by Fourier transform. In Fourier space (4.6) becomes

$$\begin{aligned} \partial_t \widehat{\eta} &= \pm\, i\Omega(k)\widehat{\eta} \\ \widehat{\eta}(0,t) &= s(t) \end{aligned} \tag{4.7}$$

where $\widehat{\eta}(k,t)$ is the Fourier transform of $\eta(x,t)$. The dynamic equation has a simple general solution,

$$\widehat{\eta}(k,t) = \alpha(k)e^{\pm i\Omega(k)t}$$

The function of $\alpha(k)$ depends on the initial data. $\alpha(k) = \widehat{\eta}(k,0)$. Therefore we have the exact solution of (4.6), that is:

$$\begin{aligned} \eta(x,t) &= \int \widehat{\eta}(k,t)e^{ikx}dk \\ &= \int \alpha(k)e^{\pm i\Omega(k)t}e^{ikx}dk \end{aligned} \tag{4.8}$$

which has to satisfy $\eta(0,t) = s(t)$. By changing the variable k into ω using the dispersion relation, $k = \Omega^{-1}(\omega)$, we obtain

$$\begin{aligned} s(t) &= \int \alpha(k)e^{\pm i\Omega(k)t}dk \\ &= \int \alpha\left(\Omega^{-1}(\omega)\right)e^{\pm i\omega t}\frac{d\omega}{V_{gr}(\Omega^{-1}(\omega))} \\ \alpha\left(\Omega^{-1}(\omega)\right) &= \breve{s}(\omega)\cdot V_{gr}\left(\Omega^{-1}(\omega)\right) \end{aligned}$$

Here, $\breve{s}(\omega)$ is the Fourier transform of $s(t)$ with respect to time. V_{gr} denotes the group velocity, given by $V_{gr}(k) = \frac{d\Omega(k)}{dk}$. By substituting α into equation (4.8) we have

$$\eta(x,t) = \int \breve{s}(\omega)e^{i(kx\pm\omega t)}d\omega \tag{4.9}$$

Secondly we will include the nonlinear term, then the signaling problem for the nonlinear dispersive AB equation becomes:

$$\begin{aligned} \partial_t\eta &= \pm\sqrt{g}A\left[\eta + \frac{1}{4}(B\eta)^2 + \frac{1}{2}B(\eta B\eta) - \frac{1}{4}(A\eta)^2 + \frac{1}{2}A(\eta A\eta)\right] \\ \eta(0,t) &= s(t) \end{aligned} \tag{4.10}$$

This nonlinear AB equation is very complicated, therefore we can not find the exact solution. We solve it numerically by Fourier transform. The results can be seen in section 4.3.

4.3 Numerical Implementation

4.3.1 Solving the Signaling Problem

In this section we will explain how we solve the signaling problem numerically. Initially we formulate the signaling problem in (4.6). Since the signaling problem has approximately the same solution as the forced equation with area generation, we solve it through the forced equation with vanishing initial elevation (see Appendix D), which is:

$$\begin{aligned} \partial_t \eta =& \pm A\eta + \gamma(x) \cdot s(t) \\ \eta(x,0) =& 0 \end{aligned} \tag{4.11}$$

where the function $\gamma(x)$ is the inverse Fourier transform of the group velocity, $V_{gr}(k) = \widehat{\gamma}(x)$. In order to solve (4.11) we transfrom it into Fourier space, which becomes:

$$\begin{aligned} \partial_t \widehat{\eta} =& \pm \widehat{A\eta} + V_{gr}(k) \cdot s(t) \\ \widehat{\eta}(k,0) =& 0 \end{aligned} \tag{4.12}$$

We solve (4.12) using the time integration procedure by ODE45 in MatLab. Using area generation means that we disturb the water to generate the wave over a certain area. This certain (generation) area represents the extent of the disturbed area and is determined by the function $\gamma(x)$. The function γ depends on the depth of the water. The deeper the water, the larger is the disturbed area. For example, we compare the $\gamma(x)$ for 1[m], 5[m], and 70[m] depth in Figure 4.1.

If we confine the generation area to the area for which $\gamma(x) > 2 \cdot 10^{-3}$, we can get the length of the area. See the skecth in Figure 4.2. For 1[m] depth the generation area is $|x| \leqslant 4$[m] and for 5[m] depth it is at $x \leqslant 19$. If the depth is 70[m], which is the case for the Draupner wave, we will get a very large generation area of approximately 400[m] ($|x| \leqslant 200$).

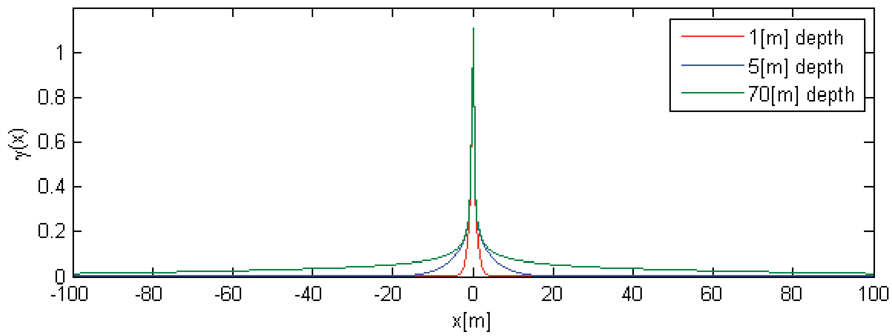

Figure 4.1: Plots of the function $\gamma(x)$ for various depths

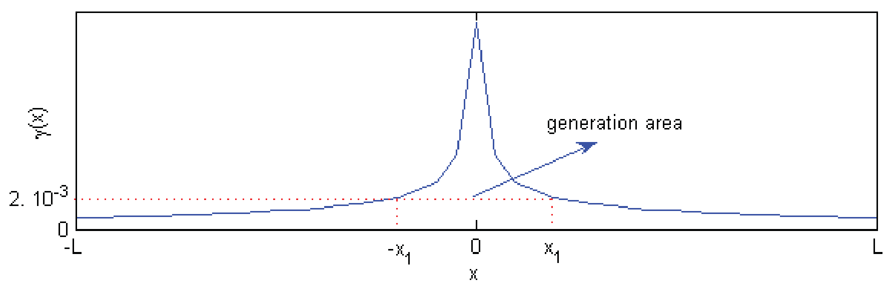

Figure 4.2: Sketch of the function $\gamma(x)$ for certain depths, showing the length of the generation area, $2x_1$

4.3.2 Numerical Data and Parameters

Here we specify the precise data that are used in the simulation of the spatial evolution of the Draupner signal.

The **Draupner wave-data** are:

- Full time signal as Figure 2.4
- $t' = [0.4688; 1200][\text{s}]$ (original time span)
- $s(t)$ (signal which we use in the numerical evolution), as plotted in Figure 2.10, but shifted and cut. The amplitude spectrum and the phases are given in Figure 2.11.
- $t = [-263.9063; 263.9063][\text{s}]$ (time span which we use in the numerical evolution)

- $dt' = 0.4688$[s] (time step of the original data)
- $h = 70$[m] (depth of the water layer)
  Figure 2.2 shows the bathymetry of North sea. According to that figure the depth of Draupner platform is approximately 70[m]. By roughly calculating the bathymetry around the location of Draupner is quite flat in an area nearby the Draupner platform.

The numerical parameters are:

- $g = 9.81$[m/s] (acceleration of gravity)
- $dt = 0.4688$ (time step of the numerical output)
  We can take any time step for the calculation output since the numerical output does not depend on dt, but it depends on dx. In our simulation, we use the same dt as the original data so that the signals at all positions have the same time step with the Draupner signal.
- $L = 1000$[m] (length of the simulation domain)
  As investigated before, the generation area for 70[m] depth is $|x| \leqslant 200$[m], therefore we should choose the length of simulation domain larger than 200[m]. In our simulation we choose 1000[m] as the total domain and 800[m] as the observed domain since the bathymetry is flat enough in radius 1000[m] and the symmetry of the Draupner wave will be observed in the interval $[0, 800]$.
- $x = [0, 800]$[m] (observed spatial domain) and damping zone = $[-100, -30]$ and $[830, 900]$ for the evolution going to the right
  The restricted domain in the simulation gives a periodic solution. The wave propagates to the right till approaching the right boundary, then it comes back to the left boundary. To avoid the periodicity we damp the wave near the boundary, so that the wave goes to zero in the damping zone (the area where we damp the wave). We damp the wave by adding $\alpha\eta$ in the right hand side of the AB equation for x in the damping zone:

$$\partial_t \hat{\eta} = \begin{cases} \pm \widehat{A\eta} + V_{gr}(k) \cdot s(t) - \beta\eta & \text{for } x \in \text{ damping zone} \\ \pm \widehat{A\eta} + V_{gr}(k) \cdot s(t) & \text{others} \end{cases}$$

The value of β determine how fast the wave decreases to zero. In order to make the wave sufficiently damped, we choose $\beta = 4$ and damping zone $= [-100, -30]$ and $[830, 900]$. This damping case is also used for the evolution going to the left.

- $x = [-800, 0]$[m] (observed spatial domain) and damping zone $= [-900, -830]$ and $[30, 100]$ for the evolution going to the left.

- $N = 2^{12}$ modes (dx approximate to 0.24[m])
  The length of ω is $\frac{2\pi}{dt}(= 13.4)$, then the maximal value of ω is 6.7. However the spectrum of signal $s(t)$ is almost vanishing for $\omega \geqslant 4$, and we restrict the frequencies until $\omega = 2$ in Figure 4.3. According to the dispersion relation, it means that the maximal wave number that is involved in the numerical calculation is $k_{max} = 1.63$. By the formula $\lambda = \frac{2\pi}{k_{max}}$, we can compute the minimum wave length, which is around 3.8[m]. For the computation, suppose we want to have 10 points in 3.8[m], then we should take the dx smaller than 0.38. Consequently we choose $N = 2^{12}$ so that $dx = 0.24$[m] ($\leqslant 0.38$).

In the next two sections we will investigate whether the symmetry property of a maximal wave is satisfied by the Draupner wave, particularly around the maximum area.

4.3.3 Simulation with the Linear AB equation

For simulation with the linear AB equation, the evolution should keep the original spectrum: the spectrum of the signal at every position is the same as original spectrum.

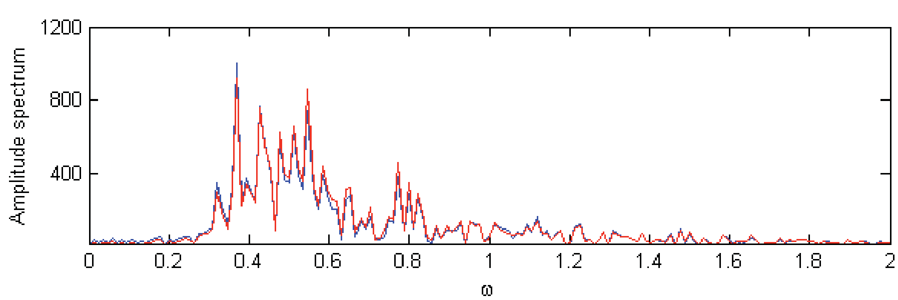

Figure 4.3: Simulation with the linear dispersive AB equation. The blue line is the original amplitude spectrum and the red line is the amplitude spectrum at $x = 20$[m]

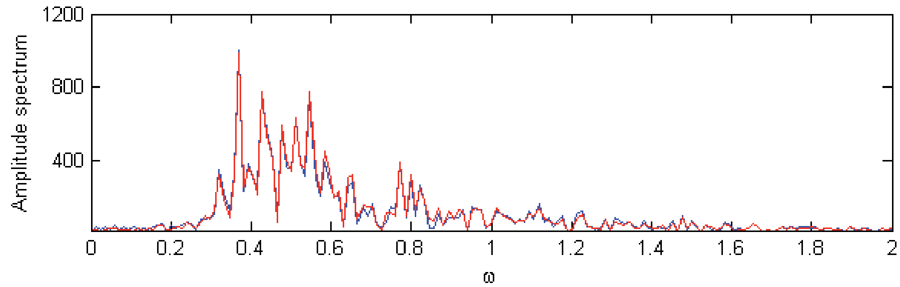

Figure 4.4: Simulation with the linear dispersive AB equation. The blue line is the original amplitude spectrum and the red line is the amplitude spectrum at $x = 200$[m]

Figure 4.3 shows the amplitude spectrum of the signal at position $x = 20$[m] and the original spectrum. These are not exactly the same. The amplitude spectrum of the signal at position $x = 20$[m] is a bit less than the original spectrum, for instance in the interval $[0.25; 0.75]$. This can be caused by two factors, a modeling and/ or a numerical factor. To investigate the numerical error, we tried the simulation by $N = 2^8$, $N = 2^{10}$ and $N = 2^{12}$. Yet, for all these choices of N, there remains an error in the spectrum which does not seem to decrease significantly with increasing N.

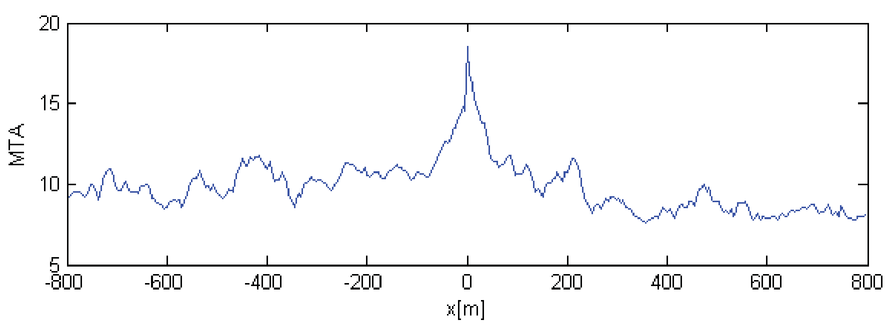

Figure 4.5: MTA of the simulation with the linear dispersive AB equation

A modeling error could be explained by the fact that the effect of the generation area is still large at position $x = 20$[m] (see Figure 4.1). As explained in section 4.3.1, for 70[m] depth the effect of the generation area is substantial for $x \leqslant 200$[m]. Therefore, we can expect a better agreement of the spectra if we catch the signal at a position $x \geqslant 200$[m]. Figure 4.4 indeed shows that the original spectrum and the amplitude spectrum at $x = 200$[m] are almost the same. A small remaining error is probably a numerical error.

Figure 4.5 shows the maximal temporal amplitude (MTA), the maximal amplitude over the time at each position for $x \in [-800, 800]$. From this figure, the maximal amplitude is at $x = 0$, but we can not be sure because the MTA around $x = 0$ is not possible to be observed precisely. This is because of the generation area, $|x| \leqslant 200$[m].

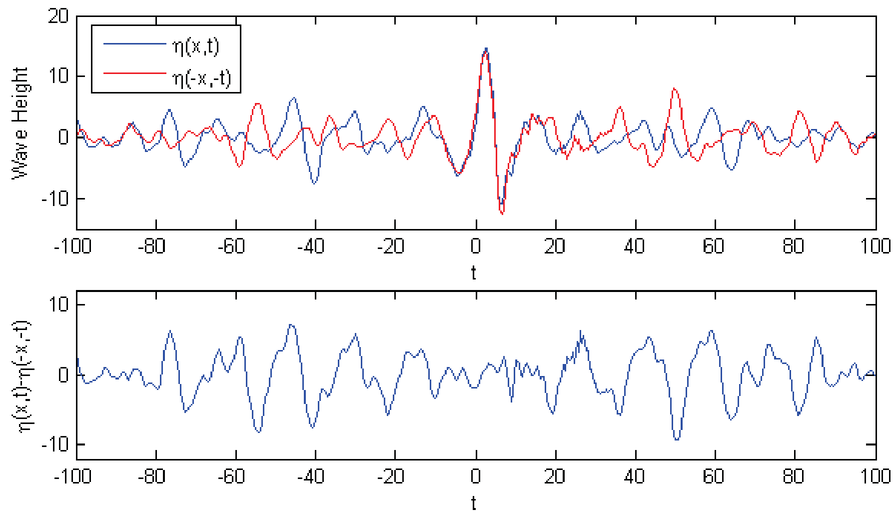

Figure 4.6: Simulation with the linear dispersive AB equation. In the upper plot, the blue line is $\eta(20, t)$ and the red line is $\eta(-20, -t)$. The lower figure is the difference $(\eta(20, t) - \eta(-20, -t))$

We show the signals of the simulation with the linear AB equation as the solution of (4.11) at various positions, $x = 20, 50, 100, 200, 400, 600$[m]. In order to see the difference between $\eta(x, t)$ and $\eta(-x, -t)$, we plot them in one figure, for instance $\eta(20, t)$ and $\eta(-20, -t)$ in Figure 4.6. We also present the plot of $\eta(x, t) - \eta(-x, -t)$ to show the difference.

As mentioned in section 4.3.2 the water depth for this simulation is 70[m]. By the dispersion relation (4.2) the phase velocity of the waves corresponding to 70[m] depth must be less than $\sqrt{70 \cdot g}$ (approximately 26[m/s]). As investigated in section 2.3 the amplitude spectrum of the Draupner signal is dominant in the range $\omega \in [0.25; 0.9]$. The $\omega = 0.25$ corresponds to the phase velocity of 25[m/s] and the $\omega = 0.9$ corresponds to the phase velocity of 10.89[m/s]. Consequently most of waves propagate with the phase velocity in the range [10.89; 25].

Numerically, we can compute the phase velocity of a wave. For instance, we will roughly compute the phase velocity of the Draupner wave. The highest peak of the Draupner wave propagates through 200[m] in about 11[s] (see Figure 4.9), i.e the velocity is approximately 18.2[m/s], corresponding to the frequency $\omega = 0.52$. This is realistic according to the depth and dispersion relation since for $\omega \in [0.25; 0.9]$, the corresponding phase velocity is in the range [10.89; 25].

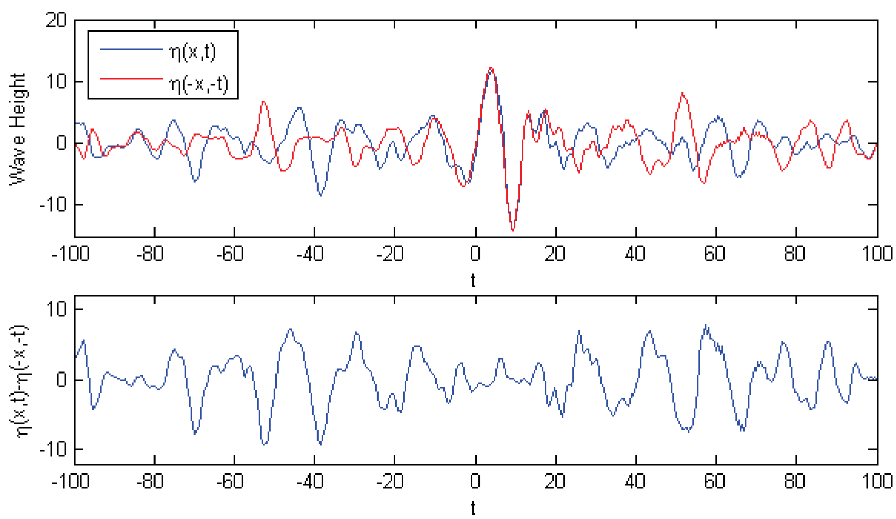

Figure 4.7: Simulation with the linear dispersive AB equation. In the upper plot, the blue line is $\eta(50, t)$ and the red line is $\eta(-50, -t)$. The lower figure is the difference $(\eta(50, t) - \eta(-50, -t))$

The signals at position $x = 20$[m], $x = 50$[m], and $x = 100$[m] show that the evolution of the maximal wave to the right and to the left are quite similar in an interval. For instance in Figure 4.7 the signals are quite similar in $t \in [-15, 19]$, but outside that range the signals become different. This means that the symmetry property is satisfied only around the highest wave. To know over which distance the Draupner wave (par-

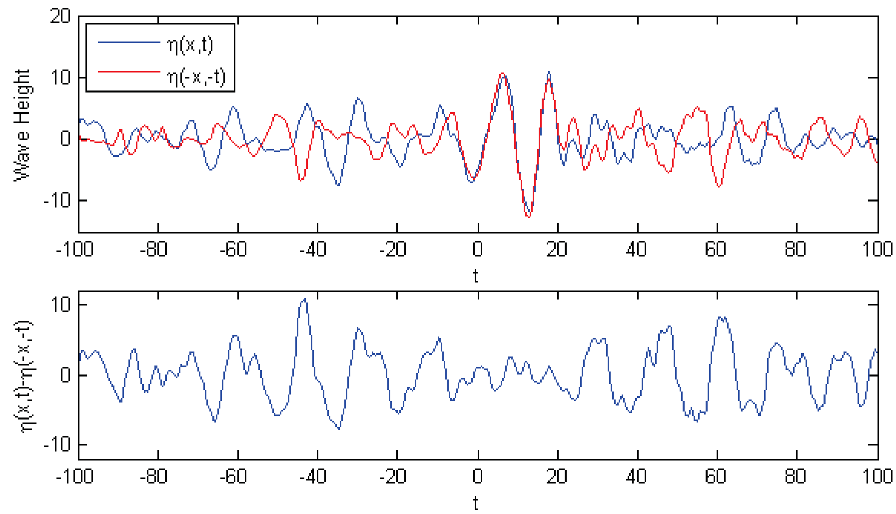

Figure 4.8: Simulation with the linear dispersive AB equation. In the upper plot, the blue line is $\eta(100, t)$ and the red line is $\eta(-100, -t)$. The lower figure is the difference $(\eta(100, t) - \eta(-100, -t))$

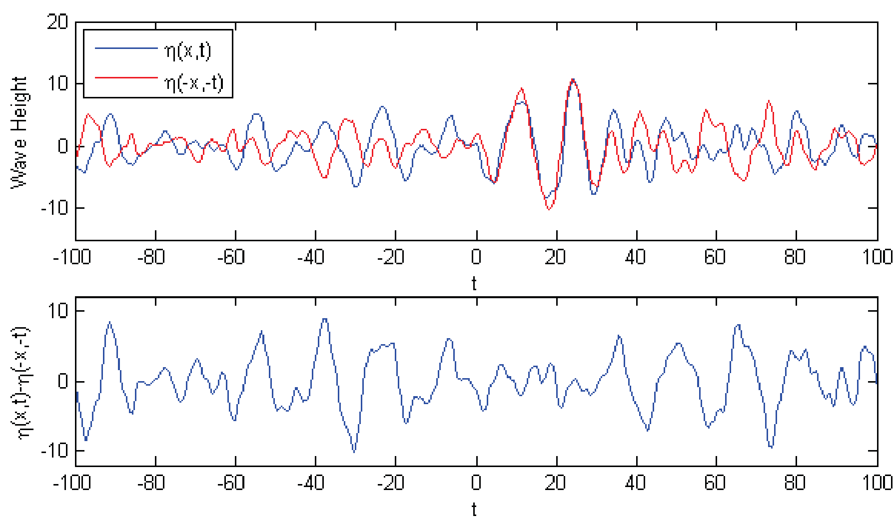

Figure 4.9: Simulation with the linear dispersive AB equation. In the upper plot, the blue line is $\eta(200, t)$ and the red line is $\eta(-200, -t)$. The lower figure is the difference $(\eta(200, t) - \eta(-200, -t))$

ticularly around highest wave) satisfies the symmetry property, the wave evolution in a long spatial interval is calculated.

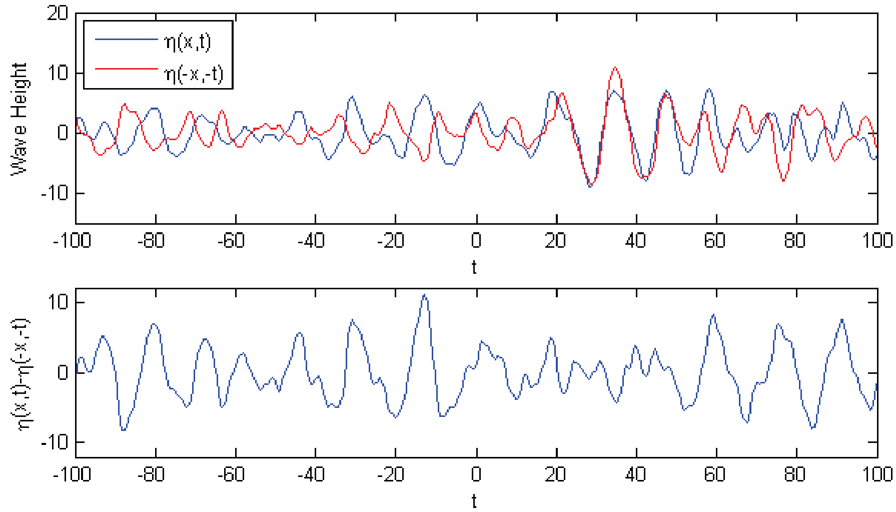

Figure 4.10: Simulation with the linear dispersive AB equation. In the upper plot, the blue line is $\eta(400, t)$ and the red line is $\eta(-400, -t)$. The lower figure is the difference $(\eta(400, t) - \eta(-400, -t))$

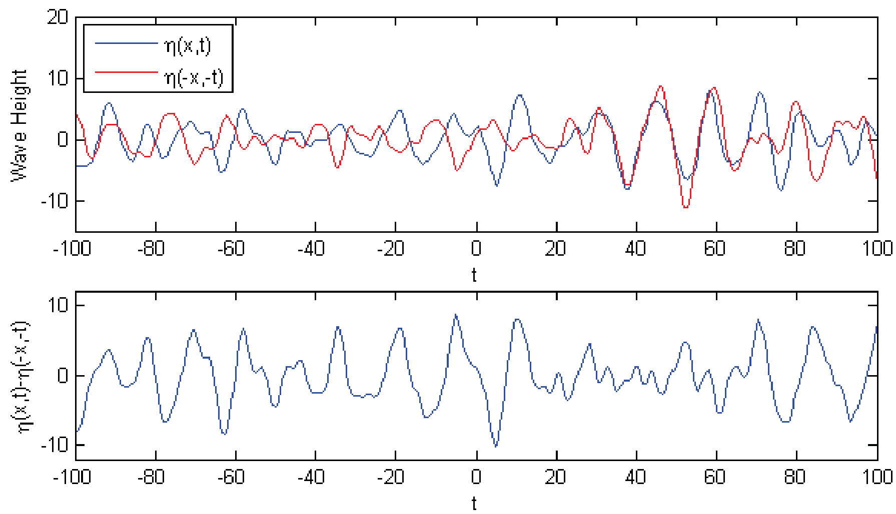

Figure 4.11: Simulation with the linear dispersive AB equation. In the upper plot, the blue line is $\eta(600, t)$ and the red line is $\eta(-600, -t)$. The lower figure is the difference $(\eta(600, t) - \eta(-600, -t))$

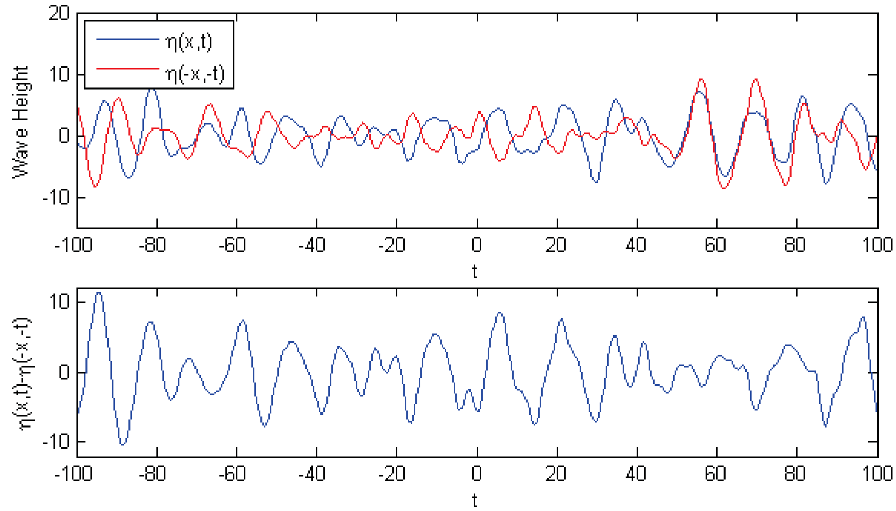

Figure 4.12: Simulation with the linear dispersive AB equation. In the upper plot, the blue line is $\eta(800, t)$ and the red line is $\eta(-800, -t)$. The lower figure is the difference $(\eta(800, t) - \eta(-800, -t))$

From these numerical results the symmetry of $\eta(x, t)$ around the highest wave is satisfied well until $x = \pm 200$[m]. For position $x = \pm 400$ and higher (Figure 4.10-4.12), the period of wave around the highest wave is still almost similar, but the amplitude of the upstream, $\eta(x, t)$ is getting larger than the downstream, $\eta(-x, -t)$, which means the symmetry property is gradually lost with increasing distance.

4.3.4 Simulation with the Nonlinear AB equation

In the simulation with the nonlinear AB equation we solve equation (4.10) in the same way as the linear case. We only add the nonlinear term of the AB equation into (4.11). The results of the simulation with the nonlinear AB equation are not different significantly from the linear simulation (see Figure 4.13 and 4.14). This also happens in the nonlinear case that the amplitude spectrum of the signal at $x = 20$[m] in Figure 4.13 is a bit different from the original spectrum and the amplitude spectrum of the signal at $x = 200$[m] in Figure 4.14 is approximately the same as the original spectrum. The difference is because of the numerical and modeling factor as explained in previous section.

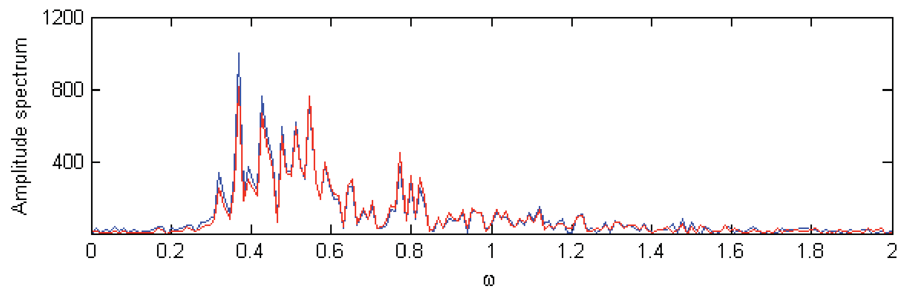

Figure 4.13: Simulation with the nonlinear dispersive AB equation. The blue line is original amplitude spectrum and the red line is the amplitude spectrum at $x = 20$[m]

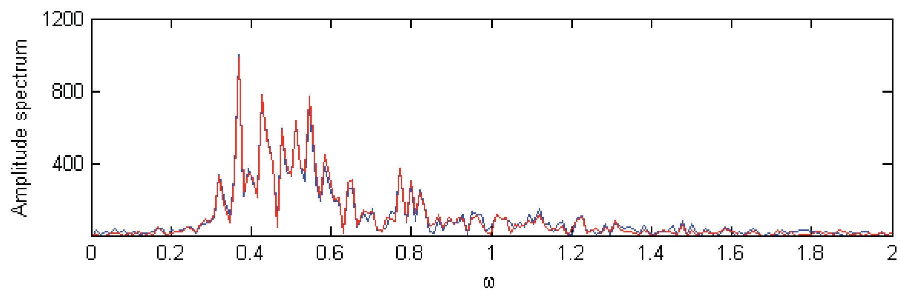

Figure 4.14: Simulation with the nonlinear dispersive AB equation. The blue line is original amplitude spectrum and the red line is the amplitude spectrum at $x = 200$[m]

Here, we present the MTA of the simulation with the linear and nonlinear AB equation in Figure 4.15, so that we can compare them. Excluding the area at $|x| < 50$, this figure shows that the nonlinear simulation gives the amplitude a bit higher than the linear one at each position x[m].

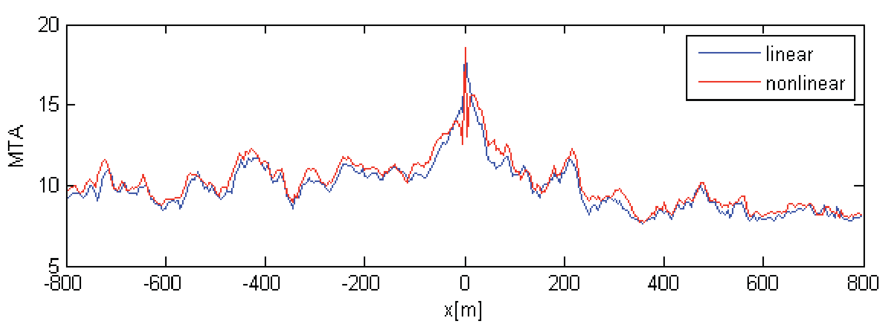

Figure 4.15: The MTA of the simulation with the linear and nonlinear AB equation

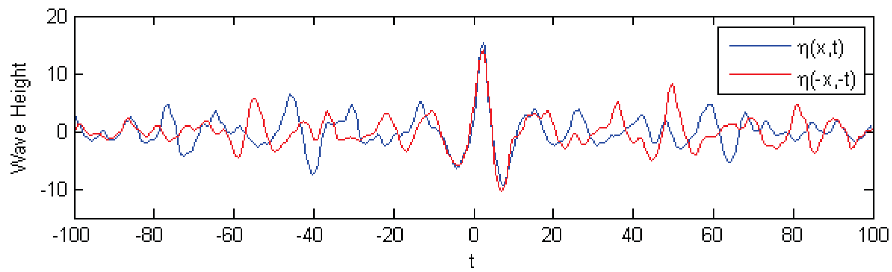

Figure 4.16: Simulation with the nonlinear dispersive AB equation. The blue line is $\eta(20,t)$ and the red line is $\eta(-20,-t)$

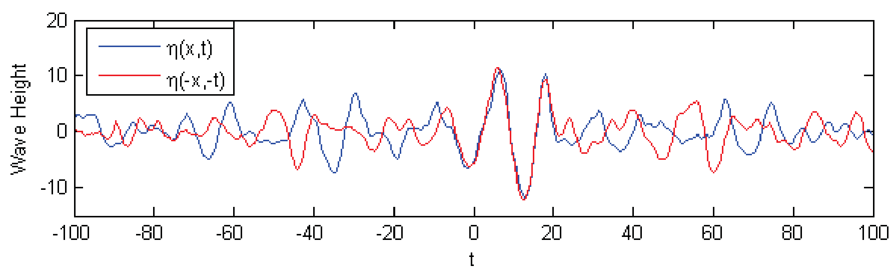

Figure 4.17: Simulation with the nonlinear dispersive AB equation. The blue line is $\eta(100,t)$ and the red line is $\eta(-100,-t)$

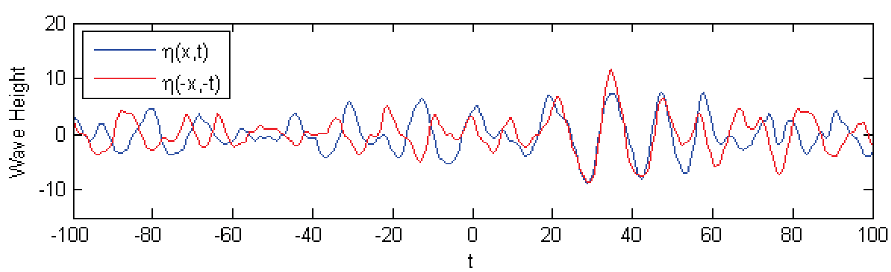

Figure 4.18: Simulation with the nonlinear dispersive AB equation. The blue line is $\eta(400,t)$ and the red line is $\eta(-400,-t)$

The signals simulated by the nonlinear AB equation at several positions are presented in Figures 4.16-4.19. The signals are not different significantly as the linear case, also for the symmetry property. We observe the symmetry property of the Draupner wave around maximum area. At $x = 20$[m] and $x = 100$[m] the maximal crest of the Draup-

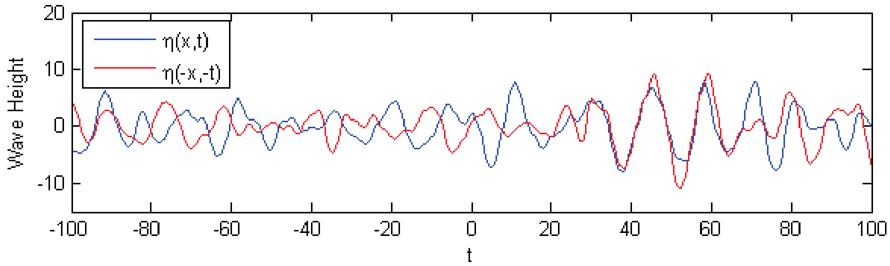

Figure 4.19: Simulation with the nonlinear dispersive AB equation. The blue line is $\eta(800, t)$ and the red line is $\eta(-800, -t)$

ner wave still keeps the symmetry property, see Figure 4.16 for $t \in (-10, 10)$ and Figure 4.17 for $t \in (0, 20)$. Figure 4.18 in the range (20,50) shows that the periods of the waves are still symmetric, but the amplitudes are somewhat different. For larger x, see Figure 4.19 the waves are only symmetric in a very small range, $t \in (35, 45)$. Furthermore, the waves gradually lose the symmetry property as distance increases.

5

Conclusions and Recommendations

This chapter will summarize our results and also give some recommendation for further investigation related to this thesis.

In this thesis we introduced the (pseudo-) maximal wave as a new concept to describe a freak wave appearance and apply it to the Draupner signal. The defined maximal wave has three properties, which are zero phases, maximal at $(x_0, 0)$, and symmetry. Our observation gives as result that the Draupner wave does not have zero phases, but random phases when we consider a large time interval around the Draupner wave. When the time interval is restricted to $[0; 528.8]$, the phases are no longer random but show some restriction. The maximal Draupner wave which is shown in Figure 3.8 has an extremely high maximal crest height. It is about twice of the maximal crest height of the Draupner wave. Therefore the maximal Draupner wave can not be an appropriate design wave to approximate Draupner wave. The appropriate one which we found is pseudo-maximal Draupner wave corresponding to $a = 0.606$ presented in Figure 3.14. Around the maximal crest it almost models the Draupner wave. The highest peak of the pseudo-maximal Draupner wave is exactly the same as the highest peak of the Draupner wave. It indicates that the pseudo-maximal Draupner wave can locally be used to describe the maximal crest of Draupner wave.

A maximal wave and a pseudo maximal wave have a symmetry property. The Draupner wave satisfies this property for t around the maximal crest. The numerical simulations with the AB equation in chapter 4 provides additional insights of Draupner wave evolution. The spatial evolution by either linear or nonlinear AB equation shows that the maximal crest of Draupner wave has the symmetry property in some approximation in a spatial domain of length about 200[m], but the symmetry property is gradually lost for increasing distance.

Future work could be to take nonlinear effects in the design of (pseudo-) maximal wave, just as has been done for fifth order NewWave. Another work is to do the spatial evolution of the Draupner signal using AB equation by point generation instead of area generation.

Bibliography

[1] Bertotti, L. and Cavaleri, L., 2008. The predictability of Voyager Accident. *Natural Hazards Earth Syst. Sci.* **8**: p. 533-537

[2] Draper, L., 1964. Freak ocean waves. *Oceanus* **10**: p. 13-15

[3] Dysthe, K. B., Krogstad, H. E., Juglard, H. S., and Trulsen, K., 2008. Freak waves, rogue waves, extreme waves and ocean wave climate. In *Proc. of Rogue Waves*, Brest, France

[4] Ferreira De Pinho, U., Liu, P. C., and Parente Ribeiro, C. E., 2004. Freak Waves at Campos Basin, Brazil. *Geofizika* **21**: p. 53-67

[5] Forristall, G. Z., 2000. Wave crest distributions: Observations and second-order theory. *J. Phys. Oceanogr.* **30**: p. 1931-1943

[6] Grigorieva, V. and Gulev, S. K., 2008. Extreme waves in visual wave observations by VOS. In *Proc. of Rogue Waves*, Brest, France. Available at `http://www.ifremer.fr/web-com/stw2008/rw/full/Grigorieva.pdf`

[7] Haver, S., 2004. Freak Waves: A Suggested Definition and Possible Consequences for Marine Structures. In *Proc. of Rogue Waves*, Brest, France. Available at `http://www.ifremer.fr/web-com/stw2004/rw/fullpapers/haver.pdf`

[8] Haver, S., 2004. A Possible Freak Wave Event Measured at the Draupner Jacket January 1 1995. In *Proc. of Rogue Waves*, Brest, France. Available at `http://www.ifremer.fr/web-com/stw2004/rw/fullpapers/walk_on_haver.pdf`

[9] Hodges, J. L. and Lehmann, E. L., 1970. Basic Concepts of Probability and Statistics. Holden-Day, San Francisco

[10] Ida, N., 2000. Engineering Electromagnetics. Springer-Verlag. New york

[11] Islas, A.L. and Schober, C.M., 2005. Predicting rogue waves in random oceanic sea states. *Phys. Fluids* **17**: p. 031701-1-4

[12] Kharif, C., Phelinovsky, E., & Slunyaev, 2005. A. *Rogue Waves in the Ocean*. Springer-Verlag, Berlin Heidelberg

[13] Marthinsen, T. and Winterstein, S.R., 1992. On the skewness of random surfaces. In: *Proc. 2nd ISOPE Conf.*, San Francisco Vol. III: pp. 472-478

[14] Massel, A.R., 1996. *Ocean Surface Waves: Their Physics and Prediction*. World Scientific Publishing, Singapore

[15] Myvroll, F. (editor). 2003. Field Measurement in Geomechanics: Proceeding of the sixth Internation Symposium FMGM. Swets & Zeitlinger BV, Lisse, The Netherlands

[16] Ojieh, N. C., Barltrop N.D.P., Xu, L., 2009. RANS Investigation of the Kinematics of an Alternative Extreme Wave. *Ocean Engineering* **36**: p. 1415-1424

[17] Ott, R. L. and Longnecker, M., 2001. *An Introduction to Statistical Methods and Data Analysis*. Nelson Education Ltd

[18] Phelinovsky, E., Kharif, C. *Extreme Ocean Waves.*, 2008. Springer Science+Business Media B.V.

[19] Rosenthal, W. and Lehner, S., 2007. Individual Wave Height of SAR. *SP-636 ENVISAT Symposium*, Switzerland. Available at http://envisat.esa.int/envisatsymposium/proceedings/sessions/2F4/461401ro.pdf

[20] Ross, S.M., 1996. *Stochastic Processes*. John Wiley and Sons Inc.

[21] Sharma, J. N., and Dean, R. G., 1979. Development and evaluation of a procedure for simulating a random directional second order sea surface and associated wave forces. *Ocean Engineering Rep.* **20**, University of Delaware, p. 112

[22] Van Groesen, E. and Andonowati, A., 2007. Variational derivation of KdV-type of models for surface water waves. *Physics letters*. Section A, **366**: p. 195-201

[23] Van Groesen, E., Andonowati, She Liam, L., and Lakhturov, I., 2009. Accurate modelling of uni-directional surface waves. *Journal of Computational and Applied Mathematics*

[24] Walker, D.A.G, Taylor, P.H., and Taylor, R.E., 2004. The Shape of large surface waves on the open sea and the Draupner New Year wave. *Applied Ocean Research* **26**: p. 73-83

[25] White , B. S. and Fornberg, B., 1998. On the Chance of Freak Waves at the Sea. *J. Fluid Mech.* **255**: p. 113-138

[26] Witham, G. B., 1974. *Linear and Non Linear Waves*. A Wiley-Interscience Publication

[27] Applied Modelling and Computation Group, Local: Bathymetry map `http://amcg.ese.ic.ac.uk/index.php?title=Local:Bathymetry_Maps`

[28] `http://www.brighton-webs.co.uk/distributions/rayleigh.asp`

Appendix A

Statistical Distribution Theory

The distribution of a stochastic variable is a description of the relative number of times each possible outcome will occur in a number of trials. It can be either continuous or discrete, but we only consider the continuous distribution. The function describing the probability that a given value will occur is called the probability function (or probability density function), and the function describing the cumulative probability that a given value or any value smaller than it will occur is called the distribution function (or cumulative distribution function). The mathematical definition of a continuous probability function, $f(x)$, is a function that satisfies the following properties:

- It is non-negative for all real x
- The probability that x is between two points a and b is

$$P(a < x < b) = \int_a^b f(x)dx$$

- The integral of the probability function is one, that is

$$\int_{-\infty}^{\infty} f(x)dx = 1$$

Since continuous probability functions are defined for an infinite number of points over a continuous interval, the probability at a single point is always zero. In the continuous case, probabilities are measured over intervals, not single point. Thus the area under the curve between two distinct points defines the probability for that interval. This means that the height of the probability function can in fact be greater than one, but the total area under the probability function is one.

Definition Let X be a random variable. For every real number x, the distribution function of a real-valued random variable X is given by

$$F_X(x) = P(X \leqslant x)$$

where the right-hand side represents the probability that the random variable X takes on a value less than or equal to x.

The probability that X lies in the interval $(a, b]$ is therefore $F_X(b) - F_X(a)$ if $a < b$. By definition the distribution function of X can be defined in term of the probability function f as:

$$F(x) = \int_{-\infty}^{x} f(t)dt$$

Every distribution function F is monotone non-decreasing and right-continuous. Furthermore, we have

$$\lim_{x \to -\infty} F(x) = 0, \quad \lim_{x \to \infty} F(x) = 1$$

The most important parameters of statistical distribution are the mean and the variance. The mean or expected value is the average of all realizations of the random process. Variance is a measure of the dispersion of a set of data points around their mean value. In other words, variance is a mathematical expectation of the average squared deviations from the mean. If a random variable X is given and its distribution admits a probability function f, then the expected value of X can be calculated as

$$\mu = E[X] = \int_{-\infty}^{\infty} x f(x)dx$$

and it has some basic properties, which are:

(1) Constant

The expected value of a constant is equal to the constant itself, i.e. if c is a constant, then $E[c] = c$.

(2) Monotonicity

If X and Y are random variables and $X \leqslant Y$, then $E[X] \leqslant E[Y]$.

(3) Linear

The expected value operator $E[X]$ is linear in the sense that

$$\begin{aligned} E[X + c] =& E[X] + c \\ E[X + Y] =& E[X] + E[Y] \\ E[aX] =& aE[X] \end{aligned}$$

(4) If X and Y are independent random variables then $E[XY] = E[X] \cdot E[Y]$
Independent means the occurrence of one event makes it neither more nor less probable that the other occurs

The variance of a random variable X with probability function f is defined by

$$\text{Var}(X) = \sigma^2 = E[X^2] - E[X]^2 = \left(\int_{-\infty}^{\infty} x^2 f(x)dx\right) - \mu^2$$

Similarly to the mean, the variance also has some basic properties, which are:

(1) Non-negative
For any random variable X, $\text{Var}(X) \geqslant 0$.

(2) The variance of a constant random variable is zero
If c is a constant, then $\text{Var}(c) = 0$

(3) The variance of a variable in a data set is 0 if and only if all entries have the same value.

(4) Variance is invariant with respect to changes in a location parameter
If a constant is added to all values of the variable, the variance is unchanged, $\text{Var}(aX + b) = \text{Var}(aX)$

(5) If all values are scaled by a constant, the variance is scaled by the squares of that constant

$$\text{Var}(aX) = a^2\text{Var}(X)$$

For the sum of N stochastic variables, $Y = \sum_{i=1}^{N} X_i$, the variance is:

$$\text{Var}(Y) = \sum_{i=1}^{N} \text{Var}(X_i) + 2\sum_{i<j} \text{Cov}(X_i, X_j)$$

in which Cov denotes the covariance. It is defined by

$$\text{Cov}(X, Y) = E[XY] - E[X] \cdot E[Y]$$

As consequence of the fourth mean property, if X and Y are independent, then their covariance is zero. Not only independent, but two random variables can also be identical. In particular cases we define some random variables which are independent and identically distributed (i.i.d). A sequence or other collection of random variables is i.i.d if each random variable has the same probability distribution as the others and all are mutually independent. Consequently they have the same mean and variance.

A.1 Uniform Distribution

In general, if all simple events X are assigned the same probability, we say that the probability model is uniform, i.e this X holds uniform distribution [9]. Uniform distribution can be discrete or continuous. Here, we only give some background about the continuous uniform distribution. The continuous uniform distribution is a family of probability distributions such that for each member of the family, all intervals of the same length on the distribution's support are equally probable. The support is defined by the two parameters, a and b, which are its minimum and maximum values. The distribution is often abbreviated by $U(a, b)$. For $a = 0$ and $b = 1$, the distribution is called a standard uniform distribution.

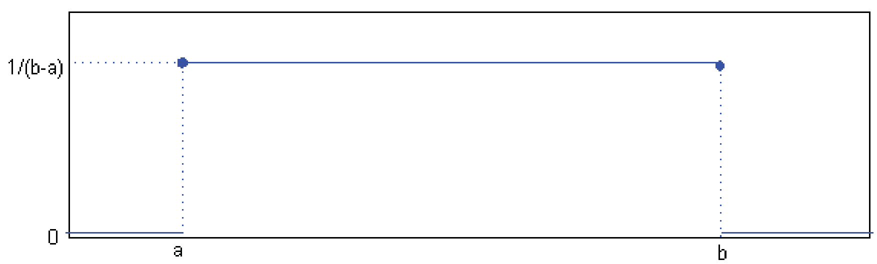

Figure A.1: The Uniform probability function

The probability function of uniform distribution is:

$$f(x) = \begin{cases} \frac{1}{b-a} & \text{for } a \leqslant x \leqslant b \\ 0 & \text{for } x < a \text{ or } x > b \end{cases} \tag{A.1}$$

The distribution function of uniform distribution is:

$$F(x) = \begin{cases} 0 & \text{for } x < a \\ \frac{x-a}{b-a} & \text{for } a \leqslant x < b \\ 1 & \text{for } x \geqslant b \end{cases} \tag{A.2}$$

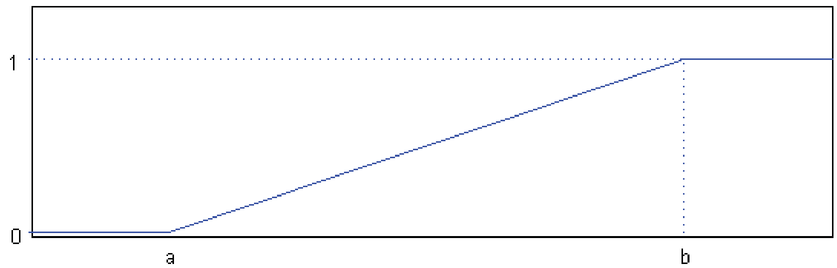

Figure A.2: The Uniform distribution function

The mean and the variance of the uniform distribution can be expressed as:

$$\mu = \frac{1}{2}(a+b)$$
$$\sigma^2 = \frac{1}{12}(b-a)^2$$

A.2 Rayleigh Distribution

In probability theory and statistics, the Rayleigh distribution is a continuous probability distribution. The Rayleigh distribution is frequently used to model wave heights in oceanography [28] (see also Appendix B). The Rayleigh probability function of the random variable X with parameter r is defined by

$$f(x;r) = \frac{x}{r}\exp\left(\frac{-x^2}{2r^2}\right) \tag{A.3}$$

for $x \in [0, \infty)$, then the probability for $x \in [a, b]$ can be computed by:

$$P(a \leqslant X \leqslant b) = \int_a^b \frac{x}{r}\exp\left(\frac{-x^2}{2r^2}\right)dx$$

Figure A.3 shows various Rayleigh distribution. From that figure we can observe that the maximum of the probability function is at $x = r$. The distribution in blue is Rayleigh(1), sometimes referred to as the standard Rayleigh distribution. The distribution function, $F(x, \sigma)$, is:

$$F(x;r) = P(X \leqslant x) = 1 - \exp\left(\frac{-x^2}{2r^2}\right) \tag{A.4}$$

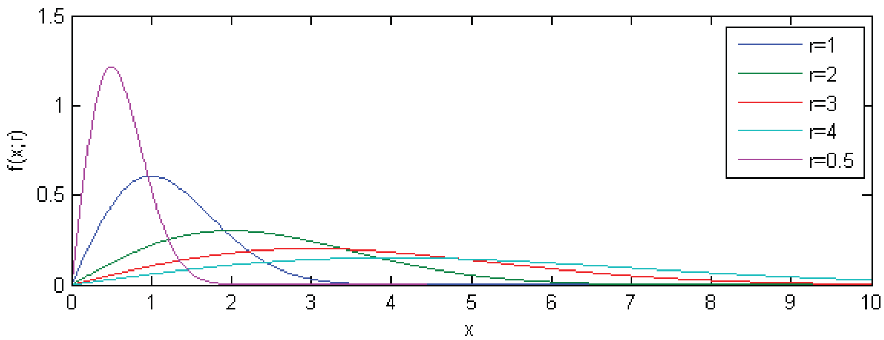

Figure A.3: The Rayleigh probability function

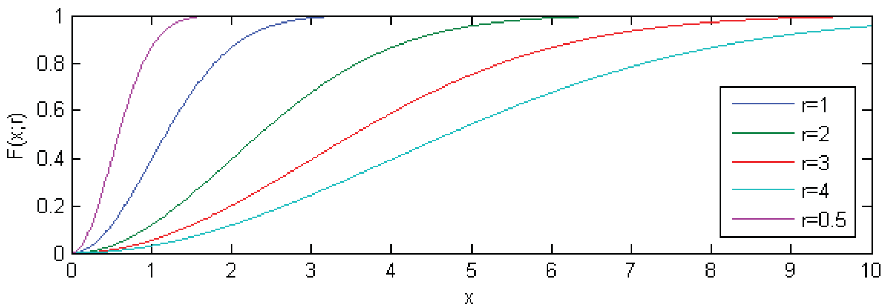

Figure A.4: The Rayleigh distribution function

The plot of the distribution function can be seen in Figure A.4. The other main properties, the mean and variance, of a Rayleigh random variable can be expressed as:

$$\mu(X) = r\sqrt{\frac{\pi}{2}} \approx 1.253r$$
$$\mathrm{Var}(X) = \frac{4-\pi}{2}r^2 \approx 0.429r^2$$

A.3 Normal Distribution

The normal distribution is also a continuous probability distribution. The continuous probability function of this distribution exists only when the variance σ^2 is not equal to zero and is given by Gaussian function:

$$f(x;\mu,\sigma^2) = \frac{1}{\sqrt{2\pi}\sigma}e^{-(x-\mu)^2/(2\sigma^2)} \tag{A.5}$$

When the variance is equal to zero, the probability function can be represented as a Dirac delta function:

$$f(x; \mu, 0) = \delta(x - \mu)$$

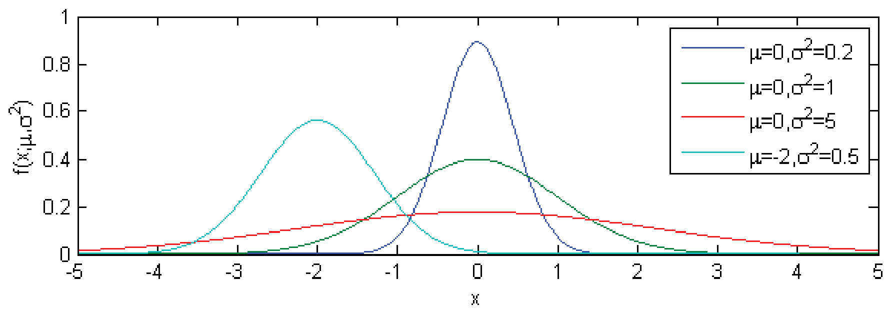

Figure A.5: The normal probability function

Characteristics features of a normal distribution are that its form in bell-shaped curve and that it is symmetric around the mean value. These characteristics can be observed in Figure A.3. The distribution function shown in Figure A.6 can be expressed as:

$$F(x; \mu, \sigma^2) = \frac{1}{2}\left[1 + \operatorname{erf}\left(\frac{x-\mu}{\sigma\sqrt{2}}\right)\right]$$

where erf is the error function defined by:

$$\operatorname{erf}(x) = \frac{2}{\sqrt{\pi}}\int_0^x e^{-t^2}dt$$

The normal distribution, also called Gaussian distribution, is the most used statistical

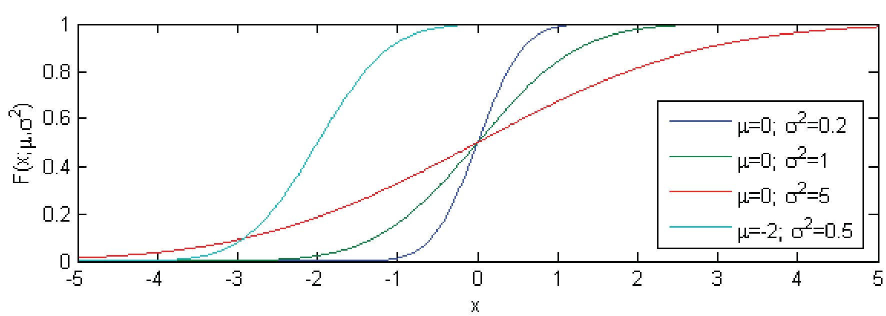

Figure A.6: The normal distribution function distribution. The principal reasons are that normality arises naturally in many physical, biological, and social measurement situations and that normal is the most important distribution in statistical inference process[17]. The normal distribution is characterized by two parameters: the mean μ and the variance σ^2. Each possible value of μ and σ^2 defines a specific normal distribution. There is a special normal distribution, so-called standard normal distribution. It has a mean zero and a variance one. All normal distributions can be transformed to standard normal distributions by the formula:

$$Z = \frac{X - \mu}{\sigma} \tag{A.6}$$

where X is the original normal distribution, μ is the mean of the original normal distribution, and σ is the standard deviation of the original normal distribution. As a result Z is a standard normal distribution.

Appendix B

Derivation of the distribution of Narrow Band process

We will show that the wave amplitude of Narrow Band process is Rayleigh distributed and the phases are Uniformly distributed in the range $[-\pi, \pi]$. We refer to [14] for the material summarized here. Consider the unidirectional wave motion of a narrow-band frequency spectrum at a given point $x = 0$. We write $\eta(t)$ instead of $\eta(0, t)$.

$$\eta(t) = \sum_n B_n \cos(\Omega_n t - \theta_n) \tag{B.1}$$

We suppose the spectrum is narrow banded with frequency Ω_m. Then we can rewrite (B.1) as:

$$\begin{aligned} \eta(t) =& \sum_n B_n \cos[(\Omega_n - \Omega_m)t - \theta_n] \cos(\Omega_m t) - \sum_n B_n \sin[(\Omega_n - \Omega_m)t - \theta_n] \sin(\Omega_m t) \\ =& A_c(t) \cos(\Omega_m t) - A_s(t) \sin(\Omega_m t) \end{aligned} \tag{B.2}$$

where

$$\begin{aligned} A_c(t) =& \sum_n B_n \cos[(\Omega_n - \Omega_m)t - \theta_n] \\ A_s(t) =& \sum_n B_n \sin[(\Omega_n - \Omega_m)t - \theta_n] \end{aligned} \tag{B.3}$$

Define $A_c(t) = B(t)\cos(\varphi t)$ and $A_s(t) = B(t)\sin(\varphi t)$ in which

$$\begin{aligned} B(t) =& \sqrt{A_c^2(t) + A_s^2(t)} \\ \varphi(t) =& \tan^{-1}[A_s(t)/A_c(t)] \end{aligned}$$

Hence

$$\begin{aligned}\eta(t) =& B(t)\cos(\varphi t)\cos(\Omega_m t) - B(t)\sin(\varphi t)\sin(\Omega_m t) \\ =& B(t)\cos(\Omega_m t + \varphi t)\end{aligned} \tag{B.4}$$

For a narrow band spectrum, the amplitude B is the amplitude of the wave envelope, which varies slowly in time. For random phases θ_n, in virtue of the Central Limit Theorem, A_c and A_s are Gaussian processes with mean value equal to zero and variance σ_η^2 as:

$$E[A_c^2] = E[A_s^2] = E[\eta^2] = \sigma_\eta^2$$

Since A_c and A_s are independent variables, the two-dimensional probability function becomes:

$$f_2(A_c, A_s) = f_1(A_c)f_1(A_s) = \frac{1}{2\pi\sigma_\eta^2}\exp\left[-\frac{A_c^2 + A_s^2}{2\sigma_\eta^2}\right] \tag{B.5}$$

Using equation (B.5) and the Jacobian of the variable transformation $J = \frac{\partial(A_c, A_s)}{\partial(B, \varphi)} = B$, we represent f_2 as a function of variables B and φ, i.e.:

$$f_3(B, \varphi) = f_2[A_c(B, \varphi), A_s(B, \varphi)]J = \frac{B}{2\pi\sigma_\eta^2}\exp\left(-\frac{B^2}{2\sigma_\eta^2}\right). \tag{B.6}$$

Observe that this probability function is independent of φ. Finally, the one dimensional probability function for amplitude B and phase φ are obtained through integration of equation (B.6), with respect to phase φ and amplitude B, respectively:

$$f_4(B) = \int_{-\pi}^{\pi} f_3(B, \varphi)d\varphi = \frac{B}{\sigma_\eta^2}\exp\left(-\frac{B^2}{2\sigma_\eta^2}\right) \tag{B.7}$$

$$f_5(\varphi) = \frac{1}{2\pi}\int_0^\infty \frac{B}{\sigma_\eta^2}\exp\left(-\frac{B^2}{2\sigma_\eta^2}\right)dB = \frac{1}{2\pi} \tag{B.8}$$

Expression (B.7) is the well known Rayleigh distribution for wave amplitude. Expression (B.8) indicates that for a narrow band process, the phases are uniformly distributed in the range $[-\pi, \pi]$.

Appendix C

Derivation of Distribution Function of $\sin(\theta_a)$ for $a \in (1/2, 1)$

The distribution function of $\sin(\theta_a)$ for $a \in (1/2, 1)$ can be computed through the sketch of the sine function. We suppose $\sin(\theta_a)$ is defined in $[-\frac{\pi}{2}, \frac{\pi}{2}]$ and we separate the domain in five intervals.

- $y < -1$
  Since $\sin(\theta_a)$ is only in the range $[-1, 1]$, it is clear that

$$F_{\sin(\theta_a)}(y) = P(\sin(\theta_a) \leqslant y) = 0$$

- $y \geqslant 1$
  It is also clear that

$$F_{\sin(\theta_a)}(y) = P(\sin(\theta_a) \leqslant y) = 1$$

- $-1 \leqslant y < \sin(-a\pi)$
  From Figure C.1, we compute the required distribution function as:

$$\begin{aligned}
F_{\sin(\theta_a)}(y) =& P(\sin(\theta_a) \leqslant y) \\
=& P(-\pi - \sin^{-1}(y) \leqslant \theta_a \leqslant \sin^{-1}(y)) \\
=& F_{\theta_a}(\sin^{-1}(y)) - F_{\theta_a}(-\pi - \sin^{-1}(y)) \\
=& \frac{\sin^{-1}(y) + a\pi}{2a\pi} - \frac{-\pi - \sin^{-1}(y) + a\pi}{2a\pi} \\
=& \frac{\sin^{-1}(y)}{a\pi} + \frac{1}{2a}
\end{aligned}$$

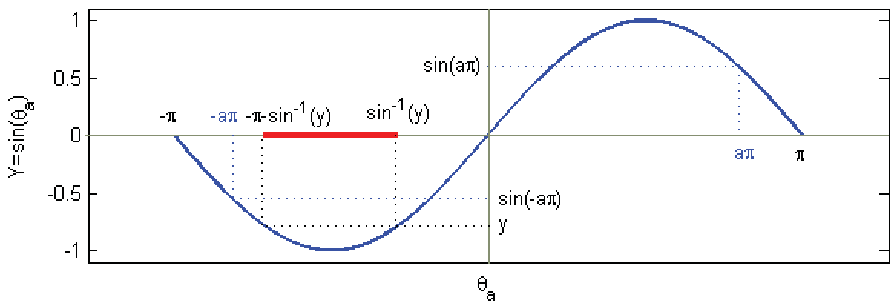

Figure C.1: Sketch for computing $F_{\sin(\theta_a)}(y)$ with $a \in (1/2, 1)$

- $\sin(-a\pi) \leqslant y < \sin(a\pi)$

  From Figure C.2, we compute the required distribution function as:

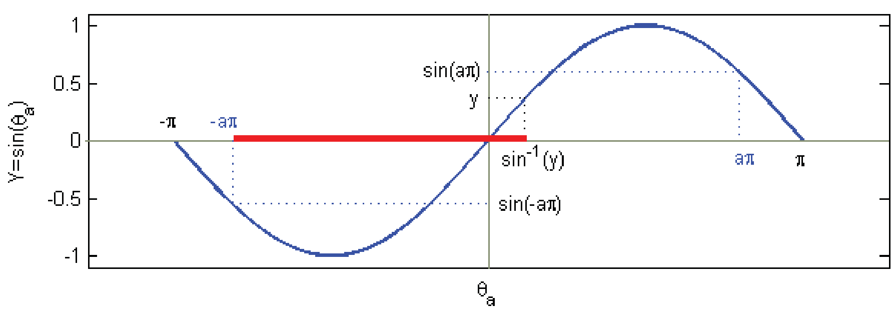

Figure C.2: Sketch for computing $F_{\sin(\theta_a)}(y)$ with $a \in (1/2, 1)$

$$\begin{aligned}
F_{\sin(\theta_a)}(y) =& P(\sin(\theta_a) \leqslant y) \\
=& P(-a\pi \leqslant \theta_a \leqslant \sin^{-1}(y)) \\
=& F_{\theta_a}(\sin^{-1}(y)) - F_{\theta_a}(-a\pi) \\
=& \frac{\sin^{-1}(y) + a\pi}{2a\pi} \\
=& \frac{\sin^{-1}(y)}{2a\pi} + \frac{1}{2}
\end{aligned}$$

- $\sin(a\pi) \leqslant y < 1$

  From Figure C.3, we compute the required distribution function as:

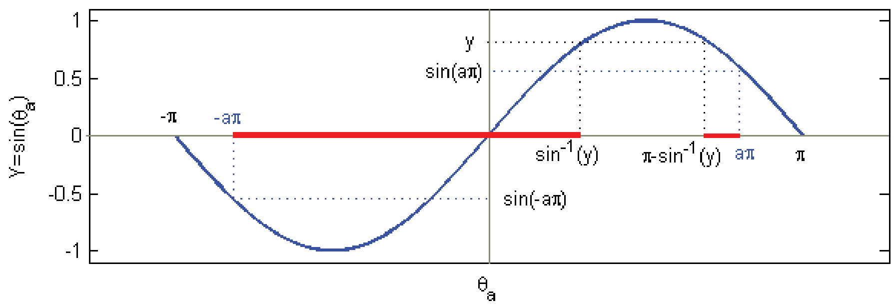

Figure C.3: Sketch for computing $F_{\sin(\theta_a)}(y)$ with $a \in (1/2, 1)$

$$
\begin{aligned}
F_{\sin(\theta_a)}(y) =& P(\sin(\theta_a) \leqslant y) \\
=& P(-a\pi \leqslant \theta_a \leqslant \sin^{-1}(y)) + P(\pi - \sin^{-1}(y) \leqslant a\pi) \\
=& F_{\theta_a}(\sin^{-1}(y)) - F_{\theta_a}(-a\pi) + F_{\theta_a}(a\pi) - F_{\theta_a}(\pi - \sin^{-1}(y)) \\
=& \frac{\sin^{-1}(y) + a\pi}{2a\pi} - \frac{-a\pi + a\pi}{2a\pi} \\
=& \frac{\sin^{-1}(y)}{2a\pi} + \frac{1}{2} + 1 - \frac{\pi - \sin^{-1}(y) + a\pi}{2a\pi} \\
=& \frac{\sin^{-1}(y)}{a\pi} - \frac{1}{2a} + 1
\end{aligned}
$$

C. DERIVATION OF DISTRIBUTION FUNCTION OF SIN(θ_A) FOR $A \in (1/2, 1)$

Appendix D

Signaling problem versus Forced equation with area generation

Here we will show our agreement in section 4.3.1 that the signaling problem has approximately the same solution as the forced equation with area generation.
The signaling problem is formulated by:

$$\begin{aligned}\partial_t \eta =& -\sqrt{g} A\eta \\ \eta(0,t) =& s(t)\end{aligned}$$

while the forced equation with area generation and vanishing initial elevation is:

$$\begin{aligned}\partial_t \eta =& -A\eta + \gamma(x) \cdot s(t) \\ \eta(x,0) =& 0\end{aligned}$$

in which A is a pseudo differential operator with $\widehat{A} = i\Omega(k) = i\omega$ and $\widehat{\gamma}(x) = V_{gr}(k)$.

The signaling problem is approximately equivalent to forced equation, since the exact solutions of those problems are approximately equal. As derived in section 4.2 the exact solution of the signaling problem is:

$$\begin{aligned}\eta(x,t) &= \int \breve{s}(\omega) e^{i(kx-\omega t)} d\omega \\ &= \int \left[\int_0^\infty s(\tau) e^{i\omega\tau} d\tau \right] e^{i(kx-\omega t)} d\omega \\ &= \int \int_0^\infty s(\tau) e^{i(kx-\omega(t-\tau))} d\tau d\omega\end{aligned}$$

This solution is not causal, because to get the solution at time t, we need all the informations of initial signal, so also the information for time in the future $\tau > t$. For this reason we use the causal expression and neglect the contribution for $\tau > t$. The signaling problem becomes approximately

$$\eta(x,t) \approx \int \int_0^t s(\tau) e^{i(kx-\omega(t-\tau))} d\tau d\omega \tag{D.1}$$

We will prove that (D.1) is precisely the solution of the forced equation.

- Substitution of $t = 0$ in (D.1) gives $\eta(x, 0) = 0$ (the initial elevation vanishes)
- By computing the derivative of (D.1) with respect to t, we show that the forced equation is satisfied:

$$\begin{aligned}
\partial_t \eta &= \int \left[\frac{\partial}{\partial t} \int_0^t s(\tau) e^{-i\omega(t-\tau)} d\tau \right] e^{ikx} d\omega \\
&= \int \left[\int_0^t -i\omega \cdot s(\tau) e^{-i\omega(t-\tau)} d\tau + s(t) \right] e^{ikx} d\omega \\
&= \int \int_0^t -i\omega \cdot s(\tau) e^{i(kx-\omega(t-\tau))} d\tau d\omega + \int s(t) e^{ikx} d\omega \\
&= \int -i\omega \cdot \breve{s}(\omega) e^{i(kx-\omega t)} d\omega + s(t) \int V_{gr}(k) e^{ikx} dk \\
&= \int -\widehat{A}\widehat{\eta} e^{ikx} dk + s(t) \int V_{gr}(k) e^{ikx} dk \\
&= -A\eta + \gamma(x) \cdot s(t)
\end{aligned}$$

- For $x = 0$ we get the required signal:

$$\begin{aligned}
\eta(0,t) &= \int \int_0^t s(\tau) e^{-i\omega(t-\tau)} d\tau d\omega \\
&= \int \breve{s}(\omega) e^{i\omega t} d\omega \\
&= s(t)
\end{aligned}$$

Acknowledgement

This thesis is the end of my journey in obtaining my Master degree in Applied Mathematics. There are many people who made this journey easier with invaluable contribution. First of all, I would like to express my sincere gratitude to my supervisor, Prof. E van Groesen. His wide knowledge and his guidance really help me in researching and writing this thesis. Thank you again for his motivation, patience, and immense knowledge.

I am grateful to Dr. Onno Bokhove and Ir. Gert Klopman for being my graduation commitee. I would also like to thank colleagues and friends in AAMP group, especially for Lie, Ivan, Wenny, and Didit. Thank you for the nice discussion. For my roommate Masoemah, thank you for the joke and the memorable conversation.

Many thanks for my Indonesian friends in Enschede for their encouragement and friendship. Special thanks for my housemates, Tettri, Dayu, and Nisa. You are my family. I do not forget to offer my warmest thanks to LUV'ers. You always make me happy and enthusiastic.

I owe my deepest gratitude to my family, Ibu, Bapak, and Mba Ika for their support and understanding. Last but not the least, my sorry and loving thanks for Mas Dedi and Gina. You are always in my heart.

May, 2010
Nida